Identification of Four Highly Conserved Genes between Breakpoint Hotspots BP1 and BP2 of the Prader-Willi/Angelman Syndromes Deletion Region That Have Undergone Evolutionary Transposition Mediated by Flanking Duplicons

J-H. Chai,[1] D. P. Locke,[3] J. M. Greally,[4] J. H. M. Knoll,[5] T. Ohta,[1,*] J. Dunai,[4] A. Yavor,[3] E. E. Eichler,[3] and R. D. Nicholls[1,2]

[1]Center for Neurobiology and Behavior, Department of Psychiatry, and [2]Department of Genetics, University of Pennsylvania, Philadelphia; [3]Department of Genetics, Case Western Reserve University, Cleveland; [4]Division of Hematology, Department of Medicine, Albert Einstein College of Medicine, Bronx, NY; [5]Laboratory of Human Molecular Genetics, Division of Medical Research, Children's Mercy Hospital and Clinics, University of Missouri–Kansas City School of Medicine, Kansas City

Prader-Willi and Angelman syndromes (PWS and AS) typically result from an ~4-Mb deletion of human chromosome 15q11-q13, with clustered breakpoints (BP) at either of two proximal sites (BP1 and BP2) and one distal site (BP3). *HERC2* and other duplicons map to these BP regions, with the 2-Mb PWS/AS imprinted domain just distal of BP2. Previously, the presence of genes and their imprinted status have not been examined between BP1 and BP2. Here, we identify two known (*CYFIP1* and *GCP5*) and two novel (*NIPA1* and *NIPA2*) genes in this region in human and their orthologs in mouse chromosome 7C. These genes are expressed from a broad range of tissues and are nonimprinted, as they are expressed in cells derived from normal individuals, patients with PWS or AS, and the corresponding mouse models. However, replication-timing studies in the mouse reveal that they are located in a genomic domain showing asynchronous replication, a feature typically ascribed to monoallelically expressed loci. The novel genes *NIPA1* and *NIPA2* each encode putative polypeptides with nine transmembrane domains, suggesting function as receptors or as transporters. Phylogenetic analyses show that NIPA1 and NIPA2 are highly conserved in vertebrate species, with ancestral members in invertebrates and plants. Intriguingly, evolutionary studies show conservation of the four-gene cassette between BP1 and BP2 in human, including *NIPA1/2, CYFIP1,* and *GCP5,* and proximity to the *Herc2* gene in both mouse and *Fugu*. These observations support a model in which duplications of the *HERC2* gene at BP3 in primates first flanked the four-gene cassette, with subsequent transposition of these four unique genes by a *HERC2* duplicon-mediated process to form the BP1–BP2 region. Duplicons therefore appear to mediate genomic fluidity in both disease and evolutionary processes.

Introduction

Prader-Willi syndrome (PWS [MIM 176270]) and Angelman syndrome (AS [MIM 105830]) are imprinted genetic disorders that arise most commonly from an ~4-Mb deletion of human chromosome 15q11-q13 (Nicholls and Knepper 2001). Molecularly, there are two common classes of deletions in patients with PWS/AS, one from breakpoint (BP) 1 to BP3 and the other from BP2 to BP3 (Knoll et al. 1990; Amos-Landgraf et al. 1999; Christian et al. 1999) (fig. 1*a*). PWS arises from the

functional loss of a set of paternally expressed genes, whereas AS is associated with the loss of maternally expressed genes. Within a 2-Mb imprinted domain distal to BP2, five paternally expressed genes encoding polypeptides have been identified; the genes include *MKRN3* (Jong et al. 1999), *NDN* (Jay et al. 1997; MacDonald and Wevrick 1997), *MAGEL2* (Boccaccio et al. 1999; Lee et al. 2000), and the polycistronic *SNURF-SNRPN* (Gray et al. 1999). This last locus also encodes five classes of snoRNAs (Cavaillé et al. 2000; de los Santos et al. 2000; Runte et al. 2001). Adjacent to the telomeric end of the paternally expressed domain are two maternally expressed genes, with loss of function of *UBE3A* underlying the neurological phenotype of AS (Jiang et al. 1998; Nicholls and Knepper 2001) and loss of the imprinted *ATP10C* locus (Herzing et al. 2001; Meguro et al. 2001) putatively associated with obesity in AS (Dhar et al. 2000; Lossie et al. 2001; Nicholls and Knepper 2001). Genes in 15q11-q13 are homologous to mouse chromosome 7C (fig. 1*a*), with the exception

of the paternally expressed *Frat3* gene, a recent evolutionary acquisition in the mouse (Chai et al. 2001). These imprinted loci in human and mouse are controlled in *cis* by a centrally located imprinting center (IC), a complex genetic element that acts bidirectionally over distances of at least 0.5–1.0 Mb to establish and/or maintain the maternal and paternal imprint (reviewed by Nicholls and Knepper 2001).

In addition to imprinted genes, several nonimprinted genes have been identified in the human and mouse PWS/AS region (fig. 1*a*). These genes may be responsible for other genetic disorders, and some of them may modify the PWS or AS phenotype. An example is the pink-eyed dilution (*p*) gene on mouse chromosome 7C and the corresponding oculocutaneous albinism type II (*OCA2*) locus in human. Although *OCA2* is recessive in humans and mice, hypopigmentation is a frequent finding in PWS and AS patients with the common deletion (Spritz et al. 1997; Nicholls and Knepper 2001). Other recessive disease loci identified within the mouse region homologous to PWS/AS are neonatally lethal cleft palate (*cp1*) due to loss of *Gabrb3* (Culiat et al. 1995; Homanics et al. 1997; Hagiwara et al. 2003) and juvenile development and fertility (*jdf2*) associated with *Herc2* gene mutations (Lehman et al. 1998; Ji et al. 1999; Walkowicz et al. 1999).

Nevertheless, the complete extent of the imprinted domain is not known in human 15q11-q13 or mouse 7C. The telomeric boundary of the 15q11-q13 imprinted domain—and corresponding region in the mouse—may be between *ATP10C* and *GABRB3*, since genetic evidence in both species indicates that the latter is not imprinted (Nicholls et al. 1993; Culiat et al. 1995; Homanics et al. 1997; Nicholls 1999; Nicholls and Knepper 2001). At the other end of the imprinted domain in humans, it has not been clear whether functional genes occur centromeric of *MKRN3*, but Ritchie et al. (1998) proposed that the imprinted domain might extend significantly farther by identifying asynchronous DNA replication at a partial duplication of the *GABRA5* locus, which maps proximal to deletion breakpoints BP1 and BP2 in the pericentromeric region of 15q11.1. Replication asynchrony is a feature of imprinted domains (Kitsberg et al. 1993; Knoll et al. 1994; Simon et al. 1999) and other domains with monoallelic gene expression (Chess et al. 1994; Hollander et al. 1998; Mostoslavsky et al. 2001). To define the extent of this imprinted domain, we searched for novel genes centromeric of *MKRN3* and describe here four unique genes in 15q11.2, the imprinting status of which was tested in human and mouse. These genes include the novel *NIPA1* (nonimprinted in Prader-Willi/Angelman syndrome 1) and *NIPA2* genes (symbols approved by the gene nomenclature committee), which encode highly conserved polypeptides with possible function as recep-

tors or transporters. Both genes—as well as the flanking *CYFIP1* (Kobayashi et al. 1998; Schenck et al. 2001) and *GCP5* (Murphy et al. 2001) genes—are candidate modulators of the PWS/AS phenotypes and/or may play a role in other disorders mapping to this region in humans and mice. Furthermore, our phylogenetic studies have identified an evolutionary transposition of these four genes from the BP3 region of ancestral vertebrates to form the human BP1–BP2 region. We propose that this transposition was mediated by the flanking *HERC2* and/or other duplicated sequences.

Material and Methods

Isolation of BAC Clones and STS Mapping of BAC and YAC Clones

The *CYFIP1* (*SRA1*) gene was identified by an *in silico* search of National Center for Biotechnology Information (NCBI) GeneMap '98. Of all EST clusters found in proximal 15q, the cluster containing the 4.4-kb cDNA KIAA0068 was the most robust, with numerous ESTs in different tissues, and was subsequently identified as *SRA1/CYFIP1* (Kobayashi et al. 1998; Schenck et al. 2001). GeneMap '98 presented compiled mapping data from two radiation hybrid panels, GB4 and G3; however, because the relative order of markers was not consistent between these panels, genes were further mapped, by PCR, to BAC and YAC contigs (see below). CITD BAC 3242E18 was identified by a BLAST search of the GenBank Genome Survey Sequence (GSS) database using *CYFIP1* cDNA sequence (GenBank accession number D38549). Exons 7 and 8 are present in the 3242E18 end sequence (AQ203319) in a $5'\to3'$ orientation compared with the end sequence. Similarly, partially sequenced BAC clones RP11-26F2 (GenBank accession number AC011767) and RP11-289D12 (GenBank accession number AC090764) were identified by BLAST with *CYFIP1* cDNA sequence and STS markers (Christian et al. 1999) *D15S18,* located in *CYFIP1* intron 1 close to exon 2, and microsatellite markers *D15S1035, D15S541,* and *D15S542* that are clustered within *CYFIP1* intron 1 ~15 kb from exon 1.

For murine *Cyfip1,* which was originally identified as *Shyc* (Köster et al. 1998), primers RN1102 and RN1103 were used to screen a Genome Systems mouse BAC library (129/Sv) by PCR, using 35 cycles at 94°C for 2 min, 55°C for 30 s, and 72°C for 1 min, with a 10-min final extension at 72°C. Mouse RPCI-22 BAC 252P22, which was identified by the PCR screen, was end sequenced, allowing a PCR product (amplified by RN1235 and RN1236) from one end of this BAC to be used to further screen the RPCI-22 BAC library by hybridization. This approach identified BACs 508F17, 402D17, 373J21, and 526E9, and BACs 466F3 and 304H15 were
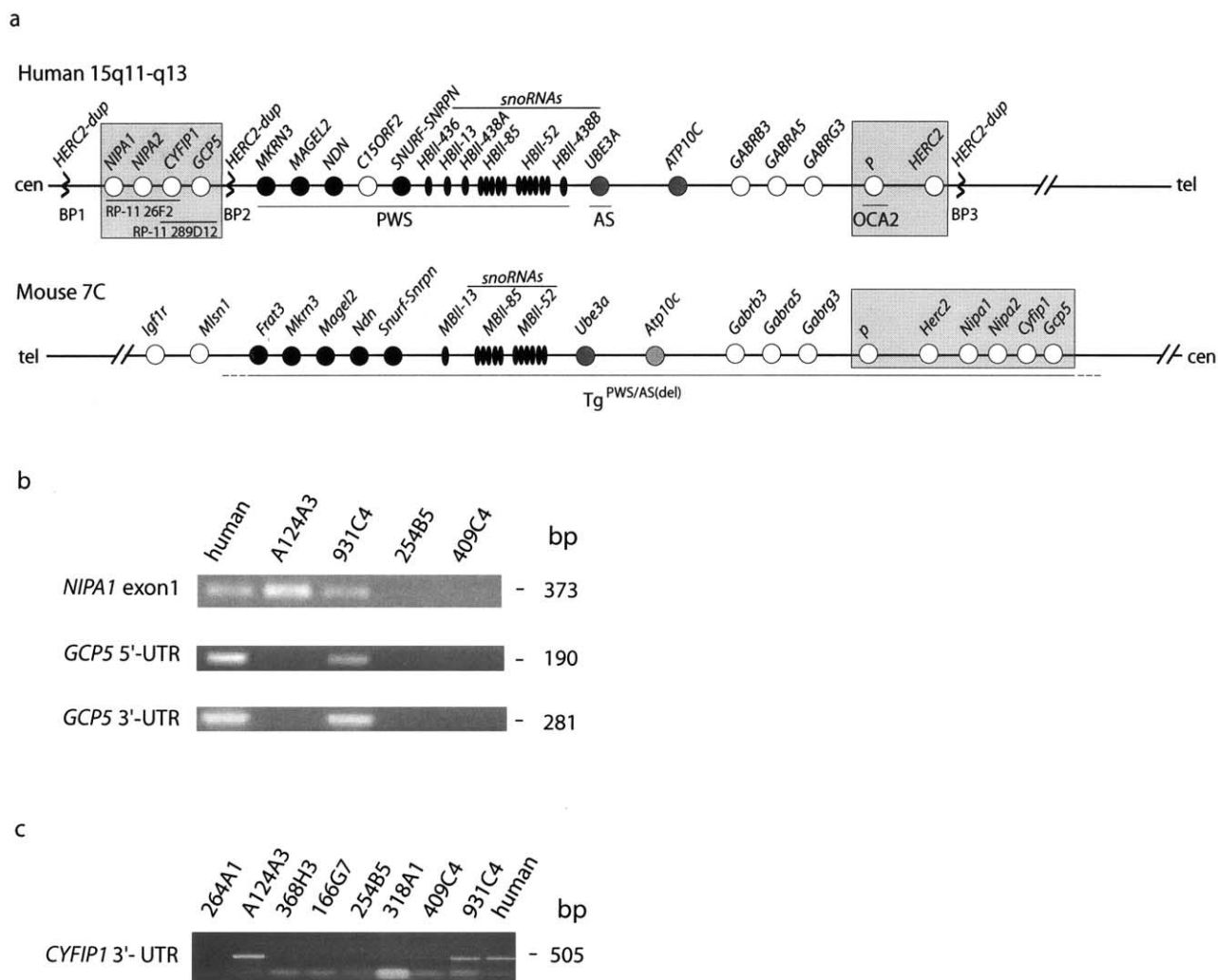
Figure 1 Genetic and physical maps. *a,* Schematic maps of human chromosome 15q11-q13 and the homologous mouse chromosome 7C region. PWS/AS deletion BP hotspots 1–3 associated with *HERC2* duplicons (dup) are shown, and the regions studied in the present work are boxed and shaded. Two BAC clones spanning the four novel BP1–BP2 genes are indicated. Black and dark gray circles represent paternally and maternally expressed imprinted genes, respectively, and white circles are biallelic, nonimprinted genes (the mouse *Atp10c* gene is likely, but not proven, to be maternally expressed [*light gray circle*]). Genes or regions associated with PWS, AS, oculocutaneous albinism type II (*OCA2*), and a transgene insertion-deletion mouse model of PWS/AS [Tg^PWS/AS(del)]] are indicated. *b,* PCR mapping of *NIPA1* and *GCP5* STS markers within YACs spanning the BP1–BP2 region. *c,* PCR detection of a *CYFIP1* STS marker in BP1–BP2 YACs. *d,* Orientation of BP1–BP2 genes, with detailed map of YACs and STS markers spanning BP1–BP2. Markers from this study are shown by large black circles, and data for the *HERC2*-dup CpG island probe (*black squares, Hin*dIII fragment sizes in kb also shown) and 254RL2 probe (*gray squares*) are from Amos-Landgraf et al. (1999). The left (L) and right (R) YAC ends (Ye), and deleted fragment (?) are also shown. *e,* Schematic of class I and II PWS and AS deletions, with detection by FISH using unique BAC clones spanning *CYFIP1*. *f,* Fine mapping and BAC contig of six nonimprinted genes in mouse 7C. Each gene is shown proportionally by the length of black arrows, with direction of transcription from 5′ to 3′. The map was determined by STS analysis derived from exons (e) and BAC ends in a series of BACs and mouse 10-kb clones (*thin black bars under genes*). Black and white squares represent STSs confirmed by PCR assay or identified by database DNA sequence analysis without further PCR assay, respectively.

identified with a PCR probe from the 195C6 T7 BAC end (table 1). BLAST searches of GSS, with the use of cDNA sequences of *Cyfip1, Nipa1, Gcp5, Herc2,* and *p*, were conducted, identifying BACs RPCI-23 (C57BL/ 6) 88I18, 452K16, 363F10, 471F18, 335K21, 49E2,

195C6, 396N13, 256L9, and 181P23 and RPCI-24 247O4, 150F2, 354P8, and 265E12. DNA from all BACs was isolated according to the minipreparation protocol recommended by Research Genetics. To establish BAC contigs and to determine gene order for the
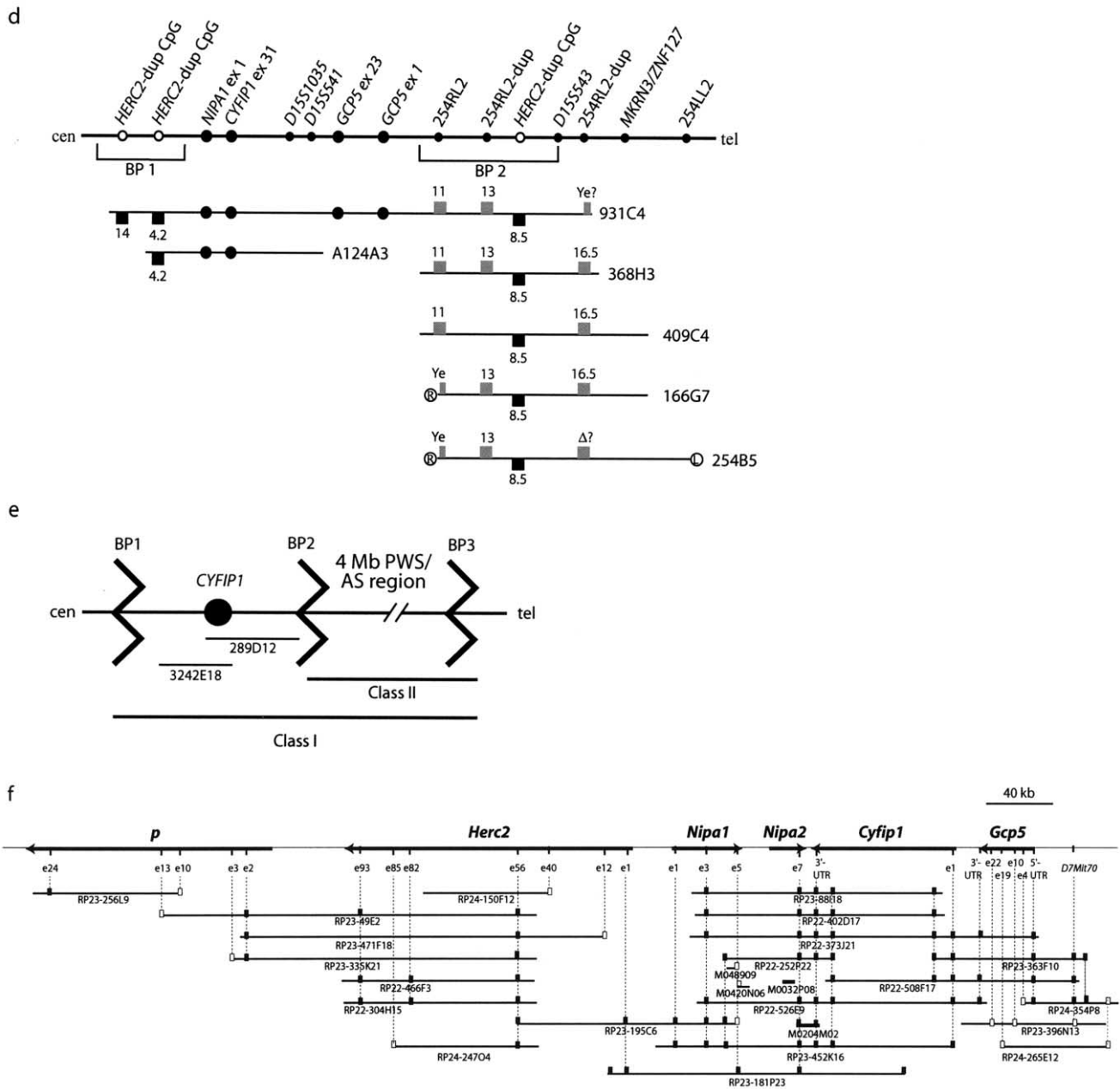
mouse loci, several pairs of primers were designed from gene exons or BAC ends (table 1). PCR was conducted under conditions of 94°C for 2 min, 31 cycles of 94°C for 30 s, 60°C for 30 s, and 72°C for 30 s and a 10-min final extension at 72°C.

DNA from YAC clones spanning the BP1–BP2 region was isolated as described elsewhere (Amos-Landgraf et al. 1999). STS primers from single exons of the *NIPA1, GCP5,* and *CYFIP1* genes (table 1) were used for PCR typing of these YACs, using 10 ng DNA for each PCR. PCR used the following cycling conditions: 94°C for 2

min, then 35 cycles of 94°C for 30 s, 55°C for 30 s, 72°C for 30 s, and a final extension for 10 min at 72°C.

FISH

For human studies, metaphase chromosome preparations were made from lymphoblastoid cell lines derived from class I and class II AS deletion patients (I: WJK29, WJK43; II: WJK18, WJK35, WJK48; Knoll et al. 1990), as well as normal individuals, according to standard protocols. BAC 3242E18 was used as the probe

Table 1

PCR Primers (5′→3′)

Position	Forward	Reverse
Cyfip1 3′ UTR (exon 31)	RN1102 ACTGATGGCATGTTTGTCTTTATG	RN1103 GCTCGTACAGATGAGTGATTTAGC
Cyfip1 exon 1	RN1389 GAGACTTGGGGAGACTTG	RN1390 GACTACAGTGGAGCAAGGA
Cyfip1 exons 4–7 (cDNA)	RN1023 CATGCTGTACACCTGGAGGA	RN1024 GCCAGGAACATGGACAGATT
CYFIP1 exons 17–25 (cDNA)	RN1213 CAGCTGTGGTTCCGAGAGTT	RN1214 TCAGCGTCTTCACGTACTGC
CYFIP1 3′ UTR	RN1021 GCATGCCTTTCTCTCCGTAA	RN1022 CCTTTCGATCTGATGTCACG
D7Mit70	RN1629 CACTTGGGGAACGTCAAGAC	RN1630 TGTAGACCATAGCCCATAAGCC
Gcp5 3′ UTR (exon 23)	RN1635 CCTGTCTAGACAATGGATTG	RN1636 GTGGTCTACTTTTATACAACTC
Gcp5 5′ UTR (exon 1)	RN1631 CATATGTTCCTGGTCTAATCAG	RN1632 GAGAGTCTTCAGACAGCTAAC
GCP5 5′ UTR (exon 1)	RN1803 GACAGGCACCAATTCGTTAG	RN1804 GTTTAGGGCGAGCTGGAAG
GCP5 3′ UTR	RN1611 CATGCCTCTAATCCCAGCAC	RN1612 GCAAGTGGTTCTTTCTGAGTC
GCP5 exons 10–11 (cDNA)	RN1609 AGCTGTTTACGATCTGTGCTG	RN1610 CAGGGTGTTAAGCAGGTGAG
Herc2 exon 1	RN1575 GTCATTTGTCGTTGCGATAG	RN1576 CTTCCAATAGAGGTAGAGTC
Herc2 exon 82	RN691 GCTCTCTTGATGAAACTGGACTCG	RN693 ACAGGCCCATGTTGGCGATCTCG
Herc2 exon 93	RN1569 CTACTTGTGGGTGCAATAG	RN792 GTCCACTAAAATGCCTCAAT
Mkrn1 (cDNA)	RN1266 TGAGAGGCCTGCCTAGGAGAG	RN1268 GCCTTGGAAAGTTGACTGCAGAG
Nipa1 exon 1	RN1432 GGCATGGGGACTGCGGCG	RN1399 CTTCTGTAGCACGAACGTG
Nipa1 exon 3	RN1401 CTGTCGCCAGATTGGAAAC	RN1402 GTACTCCAAGGGCACCTAG
NIPA1 exon 1	RN1651 CTCTTCCTGCTCCTCCCCCA	RN1653 CACCTGCGACCGCCTTCTC
NIPA1 exons 2–4 (cDNA)	RN1394 AACAGACATTGTGTGGTGGG	RN1431 ATGTTGAGCTTTTCCTTCAG
NIPA2 exons 3–6 (cDNA)	RN1384 GATTGGCTATGACCTCCAGCA	RN1386 GGAGCATGAATGACCATAACTG
Nipa2 exon 7	RN1396 TTCAGTCTCCTGTGTGAAGG	RN1397 ATCTGTGTGCTCACACAGAC
p exon 2	RN1566 CCGACTCTATAGTGAGAAACC	RN1567 GCCAAACTCTGTATGTTCAGG
p exon 24	RN1585 CTGTGATGCTCATGTCCTGC	RN1586 CCTGAACAAAGATTGGTTGC
RP22-252P22 SP6	RN1237 CCAAGAGCTAAAACTGGCAGA	RN1238 CAGCAAACCTGATGGCAGTA
RP22-252P22 T7	RN1235 GCCCAGAGACAGGGAAAATTA	RN1236 GCCCCACTGAGTCCTGTAGA
RP23-195C6 T7 (*Herc2* intron 56)	RN1511 CAATGTTGCTGCTAGCTCTG	RN1512 GAGTGTCTTCTGTGGGTCAC
RP23-363F10 T7	RN1409 CCTCCATCAGAAGTCATTGC	RN1410 GACTGAAATTGGATCCCTAG
RP24-265E12 T7	RN1613 GACAAGGTGATTAGGAGAGG	RN1614 TGCTCAAGAGCAGAGCACTC
SNURF-SNRPN exons 2–3 (cDNA)	RN420 ATCGCTTACACTTGAGAAGAACTA	RN423 CTGCTTTAACCACCTCTTGGTGTC
Snurf-Snrpn exons 3–9 (cDNA)	RN826 TCTCAGCAACAGCAAGTTCCTG	RN639 GGTGGAGGGGGTCTCATTCC

for the human chromosome FISH studies. BAC DNA was labeled with biotin or digoxigenin, by nick translation. Chromosomal hybridizations were detected as described elsewhere (Knoll and Lichter 1994; Amos-Landgraf et al. 1999). Ten to twenty metaphase cells were analyzed per cell line. To identify the chromosomal location of murine *Cyfip1,* BAC 252P22 was digoxigenin labeled and hybridized to murine metaphase chromosomes derived from Tg$^{PWS(del)}$ splenocytes, along with a mouse chromosome 7 centromere probe (kindly provided by A. G. Matera), which also hybridizes to the telomere of chromosome 5, labeled with biotin, as described elsewhere (Gabriel et al. 1999). Probes were detected by fluoroscein-labeled antidigoxigenin and Texas red avidin, with DAPI (4′,6-diamino-2-phenylindole) counterstaining.

DNA-replication–timing studies were performed as described elsewhere (Greally et al. 1998). A mouse splenocyte culture was pulsed with bromodeoxyuridine (BrdU, 100 μM) 90 min prior to harvesting. The cells were then harvested, fixed with methanol–acetic acid and spread onto slides (Henegariu et al. 2001). The BAC probes (452K16 and 252P22) were labeled by nick translation using digoxigenin, Texas red, and biotin.

FISH was performed by denaturing the slides, using 0.05N NaOH at room temperature for 4 min, followed by suppressive hybridization using probes preannealed with mouse Cot-1 DNA. The haptens were detected using antidigoxigenin-rhodamine and avidin-CY5, while simultaneously detecting S-phase cells with anti-BrdU-FITC (Pharmingen), followed by counterstaining with DAPI. Multiple image planes were acquired for each cell, to ensure that all signals were identified. Replication patterns in S-phase cells were assigned as prereplicative if a single signal was seen at a locus and were assigned as postreplicative if more than one signal was evident. The replication patterns for 50 nuclei were analyzed for each probe. For the parent of origin-specific patterns at the *Nipa1-Nipa2-Cyfip1* locus, simultaneous probing with RPCI-22 BAC 434N7 was performed with a different fluorophore on c^{32DSD} mice with a *Tyr* deletion on their paternal chromosome (Rinchik et al. 1993). The 434N7 signal from the maternal chromosome colocalized with one of the *Cyfip1* homologues in S-phase cells, allowing the confident assignment of parental origin in >90% of cells. The few cells in which the *Tyr* signal was not clearly associated with one chromosome were not included in our analyses.

Identification of NIPA1 *and* NIPA2 *cDNAs*

BLAST search of the GenBank GSS database, using *Cyfip1* cDNA sequence (GenBank accession number AF072697), matched sequence at one end of a mouse 10-kb plasmid 1M0204M02F (GenBank accession number AZ424789). The other end of this plasmid had a segment 99% identical to the *Mus musculus* hypothetical protein MNCb-2146 (renamed *Nipa2*) mRNA (GenBank accession number NM_019997; 1,867-nt sequence), 85% to several human cDNA clones (GenBank accession numbers HSU90904, BC011775, and BC000957), and 83% to a *Gallus gallus* cDNA (GenBank accession number AL588904) in the nonredundant GenBank database. A full-length human *NIPA2* cDNA (2,421 bp) spanning exons 1–7 was then assembled *in silico* on the basis of these cDNAs and partial genomic sequences from BACs 26F2 and 289D12 (see above). The cDNA sequences included one clone with exons 1 and 3–7 (2247-bp, BC011775), and one 5′ clone with exons 1, 2, 2b, and 3 (GenBank accession number BF203654). Exon 2b is a rare alternatively spliced exon in the 5′ UTR of human *NIPA2*, but it is not conserved and is likely nonfunctional. Subsequent BLAST searches confirmed numerous mouse and human ESTs with the predominant structure including sequence spanning seven exons. *NIPA2* is oriented tail to tail with *CYFIP1*, with 1,747 nt between the two genes. A *Gallus gallus Nipa2* cDNA clone (GenBank AL588904) from a chicken brain library was obtained from the Roslin Institute, United Kingdom, and was sequenced completely through the DNA Sequence Facility at the University of Pennsylvania School of Medicine. The 5′ end was from a chicken EST (GenBank accession number AJ452290). BLAST searches using human and mouse Nipa2 coding sequence in the *Fugu* Project Database identified five exons spanning the conserved ORF sequence of *Fugu Nipa2* (FT:T000059 Scaffold 59; these data were generously provided by the *Fugu* Genome Consortium for use in this publication only).

Human *NIPA1* was identified by *in silico* methods, beginning with identification, within partial BAC 26F2 genome sequence, of a second strong CpG island not associated with the 5′ end of *NIPA2*. This unique sequence matched with three human ESTs (GenBank accession numbers AW962805, AA355571, and D81972), which identify an exon-intron structure by comparison with BAC 26F2 sequence, suggesting the presence of a unique gene that further analyses identified as *NIPA1*. The AW962805 EST sequence covers part of exons 1–4 of *NIPA1*, as well as an exon termed 3b. Exon 3b is alternatively spliced (see below), but it has an in-frame stop codon, is not present in other EST clones, occurs at lower levels in RT-PCR products than does product with exons 2–4 (see below), and is not conserved in the mouse. These facts led us to conclude that exon 3b is

nonfunctional. BLAST search of the GenBank EST database also identified an initial fourth human EST (GenBank accession number BE003132), which spans part of exons 4 and 5 and the 3′ UTR of *NIPA1*, as well as three putatively orthologous mouse ESTs (GenBank accession numbers BF118592, BE654018, and BF539166). Genome sequence within BAC 26F2 that lay 3′ of the NIPA1 ORF was then used, combined with BLAST searches of the EST database, to identify numerous cDNA clones containing the two 3′ ends of *NIPA1* predicted on the basis of the mRNA size from northern blots (2.2 and 7.5 kb) and the presence of a polyadenylation signal and polyA tract at one end of the EST sequences.

The mouse BF539166 cDNA clone was purchased from Research Genetics and was sequenced to completion; it represents a full-length 1.9-kb mouse *Nipa1* cDNA. Several mouse *Nipa1* gene exon-intron boundary sequences were initially predicted on the basis of sequences identified by BLAST search of the mmtrace database and were subsequently confirmed by direct sequencing (data not shown) and by *in silico* analyses of BAC and shotgun sequence from the public genome sequence, as well as Celera databases. BLAST search of the *Fugu* Project Database with mouse NIPA1 amino acid sequence identified all five exons for the ORF sequence of the orthologous *Fugu Nipa1* (as above for *Nipa2*).

Analyses of NIPA1 *and* NIPA2 *Polypeptide Sequences*

In addition to the *NIPA1* and *NIPA2* genes identified as above for human, mouse, *Fugu*, and chicken (*NIPA2* only), using translated BLAST searches of cDNA and genome project databases, we identified an *NIPA2* ortholog in *Xenopus* (encoding a putative polypeptide of 362 amino acids), as well as a single ancestral gene in *Drosophila* (385 amino acids), *Anopheles gambiae* (351 amino acids), and *Caenorhabditis elegans* (358 amino acids), and a representative paralog in *Arabidopsis* (343 amino acids). CLUSTAL W (Thompson et al. 1994) was used to align NIPA1, NIPA2, and ancestral gene amino acid sequences, with comparison of NIPA1/2 orthologs and paralogs by an identity/similarity matrix program, while phylogenetic analyses used drawtree to plot an unrooted tree diagram. Putative transmembrane helices were predicted based on hydrophobicity plots using the TMHMM (v. 2.0) program. It may be noted that a WW protein-protein interaction domain was predicted to occur in mouse and human NIPA1 proteins; however, we assume this was a chance similarity, since it spans a strong transmembrane (TM) helix (H) domain and is not conserved.

Determination of Gene Expression by RT-PCR and Northern Blot Analyses

Total RNA samples were extracted using TRIzol (Invitrogen), according to the manufacturer's protocol, from lymphoblast cell lines derived from normal individuals, unaffected and affected patients with an imprinting defect from the PWS-U (Buiting et al. 1995) and AS-J families (Saitoh et al. 1996), and rodent-human somatic cell hybrids with a single maternal (20L-28) or paternal (A59-3az) human chromosome 15 (Gabriel et al. 1998). For the hybrids analysis, PCR primers were human specific. In addition, RNA was extracted from homogenized mouse brain from three genotypes of mice: wild-type, transgenic PWS, and AS (Tg$^{PWS(del)}$ and Tg$^{AS(del)}$), the last two of which have an ~4-Mb deletion of mouse chromosome 7C (Gabriel et al. 1999). From each sample, 1–10 μg of total RNA was pretreated with DNase I (GIBCO-BRL), with half of this used to synthesize first-strand cDNA, using SuperscriptII reverse transcriptase (GIBCO BRL) and an oligo dT primer plus random hexamers (RT+), and the other half was reverse transcriptase free (RT−). One twenty-fifth of each reaction was used subsequently for PCR amplification, with 10 mM Tris-HCl (pH 8.4), 50 mM KCl, 2 mM MgCl$_2$, 0.2 mM dNTPs, 2 U *Taq* DNA polymerase (GIBCO BRL), and 200 nM each of primers, in a 25-μl reaction volume. To assess imprinting, we utilized 35 cycles of 94°C for 2 min, 55°C–60°C for 30 s, and 72°C for 1 min, with a 10-min final extension at 72°C. Primers used for each locus (table 1) were as follows: human and mouse *NIPA1* exons 2–4; human and mouse *NIPA2* exons 3–6; human and mouse *GCP5* exons 10 and 11; human *CYFIP1* 3′ UTR, as well as exons 17–25; mouse *Cyfip1* exons 4–7; human *SNURF-SNRPN* exons 2 and 3; mouse *Snurf-Snrpn* exons 3–9; and mouse *Mkrn1*.

RT-PCR products obtained from human and mouse *NIPA1* (167 bp), *NIPA2* (339 bp), and *GCP5* (399 bp), human *CYFIP1* 3′ UTR (505 bp), and mouse *Cyfip1* 3′ UTR (258 bp, RN1102, and RN1103), as described above, were subcloned into a TA vector and used for preparation of probes. The probe for *SNURF-SNRPN* was similarly prepared from TA-cloned PCR product of exons 2 and 3 by amplification with RN420 and RN423. Probes were labeled with α-^{32}P-dCTP and were hybridized to human multiple tissue and brain multiple tissue northern blots (Clontech), human 12-lane MTN blot (BD Biosciences), or mouse multiple tissue northern blot-2 (Sigma), according to the manufacturer's protocol. β-*ACTIN* or *SNURF-SNRPN* and *Gapdh* were used as controls for human and mouse northern blots, respectively. Hybridizations were performed using ExpressHyb (Clontech) at 65°C and were washed at high stringency in 0.1 × SSC + 0.1% SDS at 60°C–65°C. Membranes were exposed to autoradiographic film at −80°C.

Results

Identification and Fine Mapping of Novel Genes in the BP1–BP2 Region of Human 15q11.2

To identify novel genes in the BP1–BP2 region, we first used BLAST searches with the chromosome 15q11.2 STS marker D15S18 and microsatellite markers D15S1035, D15S541, and D15S542 (Christian et al. 1999) to identify partially sequenced (subsequently completed) BACs RP11-26F2 and RP11-289D12, which span this region (fig. 1a). From GeneMap '98, we identified the KIAA0068 EST, subsequently recognized as *SRA1/CYFIP1* (Kobayashi et al. 1998; Schenck et al. 2001), with exons in each of the two BP1–BP2 region BACs, a location confirmed by PCR (see below). Subsequently, we identified a second gene, *GCP5* (Murphy et al. 2001), adjacent to *CYFIP1,* by BLAST searches with genomic sequence from BAC 289D12. Gene structures for these two genes have not been previously determined. The human *CYFIP1* gene spans 111.4 kb and has 31 exons (table 2) overlapping BACs 26F2 (exons 23–31) and 289D12 (exons 1–24) (fig. 1a), with short 5′ and 3′ UTRs of 52 nt and 562 nt, respectively. Exon 1 is noncoding, with the AUG start codon present at the 5′ end of exon 2. Mouse *Cyfip1* has a similar 31-exon gene structure. Human *GCP5* (also known as *TUBGCP5*) spans 46.8 kb and 23 exons with a 54-nt 5′ UTR and a 643-nt 3′ UTR (table 3), with a similar structure in the mouse (data not shown). Although 45% of the human *GCP5* 3′ UTR and 17% of the mouse 583-nt 3′ UTR are an *Alu* and a truncated B2 repetitive element, respectively, these short interspersed nuclear elements (SINEs) have different evolutionary origins and are inserted at different positions and orientations, which suggests coincidental insertion and a lack of selection on the 3′ UTR in each species. The *CYFIP1* and *GCP5* genes are arranged in a head-to-tail orientation in human and mouse (fig. 1a), with the 5′ ends of both genes associated with strong CpG islands. In addition, two novel CpG island sequences not associated with either known gene were identified from genomic sequence of BAC RP11-26F2, and these are characterized in detail below as being located at the 5′ ends of the *NIPA1* and *NIPA2* genes.

Because of the repeated nature of *HERC2*- and other duplicons in BP1 and BP2 and because of poor BAC and DNA sequence coverage in these regions, such analyses could not determine the orientation of BACs 26F2 and 289D12 or of the four BP1–BP2 region genes with respect to the centromere. Using primers derived from the 5′ end of *NIPA1* (fig. 1b), both 5′ and 3′ ends of *GCP5* (fig. 1b) and the 3′ UTR (exon 31) of the *CYFIP1* gene (fig. 1c), we performed PCR on a panel of YACs known to span the BP1–BP2 region (fig. 1d). This YAC panel was characterized previously by STS content and

Table 2

Exon-Intron Structure of the Human *CYFIP1* Gene

Exon	cDNA Position (bp)	Splice Acceptor Intron Exon[a]	Exon Size (bp)	Splice Donor Exon Intron[a]	Intron Size (bp)
1	1–46	5′ UTR	46	GCGGACGCAGgtgaggaacc	32,993
2	47–169	tatgtgttgttccagCCCAGGATGG	123	GCTCTACCAGgtgggtgccc	74
3	170–259	cttcctttccttcagCCAAATTTCA	90	CTCTAGCATGgtaatgttgc	2,062
4	260–337	tgtgttccattgcagAACGAGATGC	78	CATCCCACAGgtgccacgct	197
5	338–439	ttcctttattcccagGTGAAATGTA	102	GTACTTCCAGgtaaaatggc	1,198
6	440–621	gcttcctctgcacagAGAAATGCCA	182	CGTACAAGAGgtgagcaccc	3,660
7	622–718	tttttgttttcaaagGGCCGCTCAG	97	GATCACACAGgtaaggctgg	85
8	719–847	tgctctgtgtttcagTCTCTGCAGC	129	GCTTCTCAAAgtacgtgtgt	1,979
9	848–952	tttgtggcttttcagGTCATGGGAT	105	GTACTTCAAGgtgagttaca	3,212
10	953–1,044	gttctttgaatacagCAACTCCAGG	92	ATAAATCTCGgtaggaggag	1,460
11	1,045–1,162	tttctctctgcacagATGGACGTGC	118	CAACAGCGAGgtcgccccgc	4,185
12	1,163–1,285	gcccgccttgtgcagGTGGTCACGG	123	GATGGAAGTGgtaggccccg	1,797
13	1,286–1,411	tttcggccaccacagTATTCCTGGA	126	CCTAGTGGAGgtgaggatgc	7,115
14	1,412–1,578	ctgtgtcccccgcagGTGATCGCCA	167	TCATCCAGAGgtcagccttc	753
15	1,579–1,726	tggtggggtgttcagTGTCCTGCAG	148	CAGCACTCAGgttctcgtcc	1,152
16	1,727–1,880	ccttggataatccagCTTTACATGG	154	AATTTCAGTGgtaagagata	1,593
17	1,881–2,037	tttgaaccctcccagAAACGCTGCA	157	CGATGATGGAgtgcgtgtcc	2,437
18	2,038–2,134	tgctgtcctctgcagGTACGTGCTC	97	TGAGGCCGAGgtgaggcccc	1,354
19	2,135–2,211	tttctttttcttcagGTGAATCTAT	77	TGGCAGGAAGgtgagtatct	105
20	2,212–2,320	ttccttctacactagTTTGCTTCTT	109	GCATGTGCAGgtgagctggg	1,201
21	2,321–2,440	ccctgtgtacgccagCTCCTCGGCA	120	CTCCATAGTTgtaagtaatt	5,287
22	2,441–2,640	tctttggtgccacagGAGCTGGATG	200	CTACCAACCGgtgagcgtgc	10,723
23	2,641–2,728	atctttcttgtttagGTTTGTTCGG	88	TGGATCCAAGgtaggctcca	9,878
24	2,729–2,872	tgccctgttttccagGCTTTGAACT	144	CAAGAGCCTGgtgagtgttc	932
25	2,873–2,963	tcatctcccggcagCTGCAAGGCA	91	GGCTCTCCTGgtgagtgcgg	1,703
26	2,964–3,094	ctcccgccaccgtagGTATCCTGGA	131	GCAGAGCCTGgtgagtggcc	4,642
27	3,095–3,167	ctttctctgctctagTCTTTAGAAG	73	CATGTGAAAGgtgagcctgc	475
28	3,168–3,262	tttttctactgcagAGGGGGAGAG	95	GACCCCTCAGgtaacgtgta	821
29	3,263–3,501	ttgtcctttctgcagCAAATTGCCA	239	TCACAGTCGAgtaagtgtgt	1,340
30	3,502–3,649	gcttcttgttcctagGCAGTGCTTT	148	TAAAAATGTGgtatgtggat	2,633
31	3,650–4,376	ctttgatggttgtagCCTTTGAAGA	727	3 UTR (3818–4379)	NA[b]

[a] Lowercase letters refer to intron sequences, and uppercase letters refer to exon sequences. Underlined letters "ag" and "gt" represent consensus splice acceptor and donor sequences, respectively. The underlined "AGT" represents the sequence coding for the translation initiation codon in the corresponding mRNA.

[b] NA = not applicable.

HERC2-duplicon mapping (Amos-Landgraf et al. 1999). Both *NIPA1* exon 1 and the 3′ UTR of *CYFIP1* were detected on YACs 931C4 and A124A3 (fig. 1b, c, and d), confirming that these genes map proximal to BP2 of *MKRN3* and were therefore proximal to the known PWS imprinted domain. Furthermore, both ends of *GCP5* are within YAC 931C4 but not A124A3 or any BP2 region YACs (fig. 1b and 1d), unambiguously defining the order as cen–*NIPA1*–*CYFIP1*–3′-*GCP5*-5′–BP2–tel.

FISH Mapping of BP1- and BP2-Associated Rearrangements

BAC clone 3242E18, containing exons 7–31 of *CYFIP1* from the BP1–BP2 region (fig. 1e), was utilized for FISH studies on metaphase chromosomes from three normal human lymphoblastoid cell lines, with hybridization to a single region of proximal chromosome 15 in band 15q11.2 (fig. 2a). No other chromosomal hybrid-izations were detected, including in interphase cells, confirming that BAC 3242E18 does not contain duplicon sequences. Therefore, we investigated the pattern of hybridization of BAC 3242E18 against a panel of cell lines from patients with AS deletions. Deletions in patients with AS and PWS (fig. 1e) are either class I, which extends from BP1 (15q11.2) to BP3 (15q13), or class II, which extends from BP2 (15q11.2) to BP3 (Knoll et al. 1990; Amos-Landgraf et al. 1999). As expected, the 3242E18 FISH assay distinguishes class I and class II deletions in patients with AS, because the BAC is present on both chromosomes 15 in cells of three class II patients and is present only on the normal chromosome 15 in cells from two class I patients (fig. 1e; data not shown).

Physical Map Spanning Six Genes at the Centromeric End of Mouse Chromosome 7C

The human *CYFIP1* gene is orthologous to the mouse *Shyc* (*Cyfip1*) gene (Köster et al. 1998; Schenck et al.

Table 3

Exon-Intron Structure of the Human *GCP5* Gene

Exon	cDNA Position (bp)	Splice Acceptor Intron Exon[a]	Exon Size (bp)	Splice Donor Exon Intron[a]	Intron Size (bp)
1	1–200	5′UTR (1-54)	200	CCAACTTCAGgtgtggggcacg	2,244
2	201–254	tgtctttaatagATTTCATCGT	54	CAATCGAAGGgtatgccttcaa	92
3	255–363	cttatattttagAATTTATGAA	109	GGAAATAAAGgtatgccttcaa	4,075
4	364–460	tttgttttaaagACAGATGCAC	97	AAAGAAGTGGgtatgttactag	696
5	461–540	gttacattagAAAAGAAAGA	80	GGACACACCAgtaagtggtagt	928
6	541–675	tttttaaatcagAATTGGTCTG	135	AGTTGGAAAGgtattatgtgtt	3,582
7	667–791	cagatgagccagATGAGCCAGA	125	CTGCTGTCTGgtaagaagctaa	985
8	792–881	gctgtctcatagGGACCAACAC	90	AAACCCTATGgtaagaaatgtt	1,284
9	882–975	atctcatttcagGTTACTTTCA	94	TTTAACACATgtaagttatttg	542
10	976–1,222	cttgtgttgtagAGCTGTTTAC	247	ATCAATAATGgtattaaatgtt	1,784
11	1,223–1,425	tgatatttgcagATACTACAAT	203	TGAGCAAACCgtaagtgagact	2,623
12	1,426–1,539	tctctgcctcagGTCTCCCTCC	114	TCATCCAGAGgtgagctgcagc	7,177
13	1,540–1,809	gaatctctttagAAACAAAAAT	270	GGAGCCAGAGgtacttgttccg	6,824
14	1,810–2,009	tttatgtttcagATGCAGAAAG	200	ACTTTGCAAGgtgagacacacc	998
15	2,010–2,198	ttttatcttgagGATGTATTTG	189	AAGATTACAGgtaaaagagtaa	1,063
16	2,199–2,381	ctctccattcagGTTGGTAGAA	183	ATAGTTCACAgtaaaatatgga	2,348
17	2,382–2,466	ttctttctttagTCTATCTATA	85	CAGCTACAAGgtatatgctgat	94
18	2,467–2,587	tttgtttcatagGTCCCATGGC	121	CTTTTTGGTGgtaagatttgtt	440
19	2,588–2,766	aatgttttatagAACTGGTTAG	179	CATGACCAGGgttttgtgcctct	1,203
20	2,767–2,892	ttctcttccaagATTCTACACA	126	GAGAGAAAAGgtacatgagatg	947
21	2,893–2,981	tttggtctgcagGTCAGCTTTG	89	GCACTTGGCGgtaagtatgtga	2,394
22	2,982–3,082	ttttattcctagAATGGAATCT	101	TTTCCCCATTgtgagtatatca	701
23	3,083–3,771	ttcttcccacagTGGAATCTCT	689	3′ UTR (3127–3771)	NA[b]

[a] Lowercase letters refer to intron sequences, and uppercase letters refer to exon sequences. Underlined letters "ag" and "gt" represent consensus splice acceptor and donor sequences, respectively.

[b] NA = not applicable.

2001). We isolated the *Cyfip1* 129/Sv RPCI-22 252P22 BAC clone (fig. 1*f*) by PCR screening with a 3′ UTR STS. FISH was then performed on metaphase chromosomes from a mouse model of PWS with a chromosome 7C deletion (Gabriel et al. 1999). BAC 252P22 (*Cyfip1*) localizes to the normal chromosome 7C region and within the mouse transgene-induced deletion (fig. 2*b*), which expands the known syntenic relationship between human 15q11-q13 and mouse 7C (fig. 1*a*).

To generate a physical map, seven unsequenced 129/Sv and 14 partially sequenced C57BL/6 BACs were identified (see "Material and Methods" section) and typed by PCR with STSs derived from the *p, Herc2, Nipa1, Nipa2, Cyfip1,* and *Gcp5* genes and with BAC end sequences created in this study, allowing generation of an overlapping BAC contig map (fig. 1*f*). These data indicate that the genes in this region are arranged in the order cen–*Gcp5*–*Cyfip1*–*Nipa2*–*Nipa1*–*Herc2*–*p*–tel (fig. 1*f*). The map is anchored at one end by an STS marker, D7Mit70, which maps close to the *l71Rl* locus involved in peri-implantation survival (Wu et al. 2000), that is ~22 kb centromeric to *Gcp5*.

Replication Analyses of the Nipa1-Nipa2-Cyfip1 *Locus*

Replication-timing studies of imprinted regions have demonstrated a parent-of-origin–dependent asynchrony,

using FISH and quantitative PCR techniques (Kitsberg et al. 1993; Knoll et al. 1994; Simon et al. 1999). For two BACs of different sizes that collectively span the *Nipa1, Nipa2,* and *Cyfip1* genes, we see a pattern of asynchrony that is similar to that at the imprinted *Mkrn3* and *Snurf-Snrpn* loci (fig. 2*c*). To test whether the pattern at *Nipa1-Nipa2-Cyfip1* was determined by parent of origin, we used mice heterozygous for a deletion at the mouse *Tyr* (*c*) locus (*c*[32DSD]) (Rinchik et al. 1993) to examine which chromosome was replicating earlier in each cell. The relatively close linkage of *Tyr* to the imprinted 7C region (~14 cM) makes this a useful marker for in situ studies of this region while being sufficiently distant that the likelihood that *cis* effects of the deletion cause disruption of imprinting is very small. We found a pattern of replication in these cells that was asynchronous but was not due to parent-of-origin influences. In other words, the proportion of cells that showed the paternal chromosome replicating early was equal to the proportion that showed the maternal chromosome replicating early (fig. 2*c*).

Characterization of the NIPA1 *Gene in Vertebrates*

Human *NIPA1* maps within BAC 26F2 and was identified, on the basis of a strong CpG island, by visual inspection of genomic DNA sequence, followed by
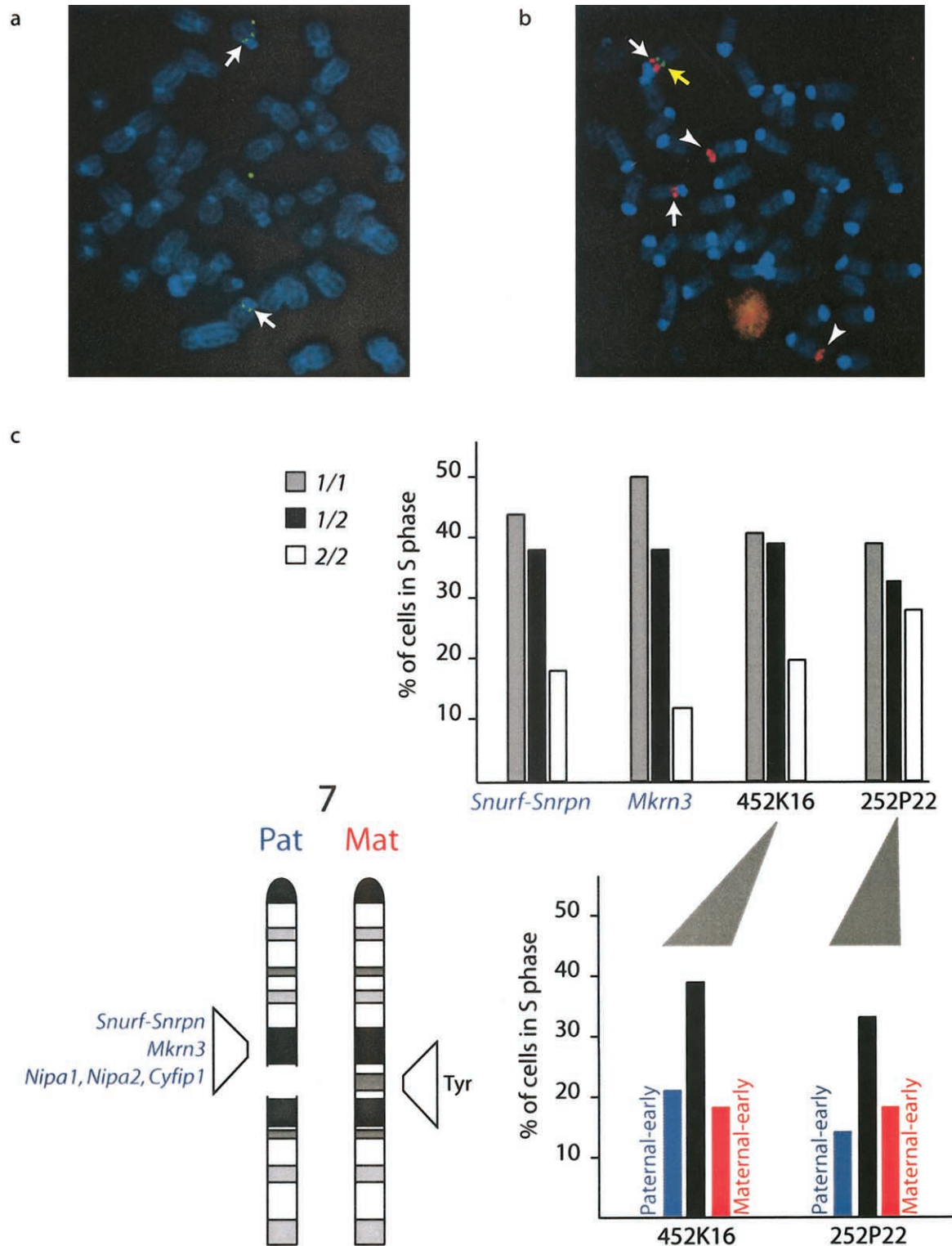
Figure 2 FISH mapping of *CYFIP1* in human and mouse, as well as DNA replication-timing asynchrony at the mouse *Nipa1-Nipa2-Cyfip1* locus. *a*, BAC 3242E18 spanning *CYFIP1* (fig. 1*e*) is unique and maps to human chromosome 15q11.2 (*arrows*). *b*, BAC 252P22 (fig. 1*f*) maps to mouse chromosome 7C (*green signal, yellow arrow*) in metaphase chromosomes from Tg^PWS(del) mice. A control probe identifies the chromosome 7 centromere (*red signal, white arrow*) but also hybridizes to the telomere of chromosome 5 (*white arrowhead*). *c*, Probes from imprinted (BACs RP-23 371M8 and 266F22 for *Snurf-Snrpn* and *Mkrn3*, respectively) and nonimprinted (BACs 452K16 and 252P22 for *Nipa1-Nipa2-Cyfip1*; see fig. 1*f* and fig. 5) loci exhibit asynchronous replication (a high singlet/doublet [1/2] proportion of hybridization foci in S-phase cells, comparable to prior studies [Kitsberg et al. 1993; Greally et al. 1998; Simon et al. 1999]).

assembly of a cDNA sequence contig, using BLAST searches extending 3′ from the CpG island (see "Material and Methods" section for details). This led to an *NIPA1* cDNA sequence of 2,247-bp that spanned five exons and 38.8 kb in genomic DNA (fig. 3*a*) and encoded a putative polypeptide of 329 amino acids (fig. 4*a;* see below). The five *NIPA1* exon-intron boundaries conform to consensus splice acceptor and donor sequences (table 4), with the translational AUG start codon present in exon 1, the stop (TGA) codon in exon 5, and in the 3′ UTR an ATTAAA variant polyadenylation signal at cDNA position 2221–2226 (fig. 3*a;* table 4). Although single base changes of the hexanucleotide (AATAAA) poly(A) signal sequence greatly reduce polyadenylation, the A→T substitution at position +2 of the noncanonical ATTAAA hexamer is the mildest mutation and corresponds to the most common variant (Sheets et al. 1990). Nevertheless, multiple *NIPA1* ESTs have polyA tails beginning 13–17 nt 3′ of this polyA signal, suggesting this as a bona fide 3′ end of low-abundance *NIPA1* transcripts, which was supported by northern analysis of gene expression, although these studies also identify a larger neuronal transcript (see below). Therefore, we examined genomic sequence further 3′ both visually and by BLAST against the EST database, which allowed identification of the major human *NIPA1* 3′ UTR polyadenylation signal (AATAAA) at cDNA positions 6540–6545. The latter is embedded in a region that is highly conserved in five eutherian mammals and that is diagnostic for the *NIPA1* 3′ end (fig. 3*b*).

Within the GC-rich (75%) exon 1 of *NIPA1,* we identified a (GCG)$_n$ repeat, encoding polyalanine (fig. 4*a*), which we examined for polymorphism by one or both of following methods: direct sequencing of exon 1 PCR products or detection of PCR products by use of a ^{32}P–dCTP labeled primer. This analysis showed polymorphism in 135 chromosomes of European and Asian origin with the number of repeats ranging from 6 to 10 (data not shown). The two most frequent alleles, (GCG)$_8$ and (GCG)$_7$, have allele frequencies of 0.78 and 0.2, respectively. Additional studies are needed to determine whether expansions occur in the *NIPA1* (GCG)$_n$ repeat and are disease associated.

The mouse *Nipa1* cDNA was identified by *in silico* methods, using the human coding sequence as well as sequencing of a 1.9-kb cDNA clone. By comparison with mouse genome sequence, the *Nipa1* locus was found to span 41.1 kb of genomic DNA and to include five exons that are highly conserved with the human *NIPA1* gene (fig. 3*a;* table 4). Mouse *Nipa1* encodes a putative polypeptide of 323 amino acids (fig. 4*a*), with an N-terminal polyalanine sequence encoded by a (GCG)$_3$ GCT(GCG)$_3$ sequence in exon 1. In a manner similar to that in humans, two polyadenylation signals occur in the mouse *Nipa1* 3′ UTR at cDNA positions 1866 nt and 6840 nt

of the cDNA (fig. 3*a*), both of which are AATAAA signals and correspond to the two *Nipa1* transcripts (see below). We also identified *in silico* the complete orthologous *Nipa1* gene from the *Fugu* Project Database by translated BLAST analyses, using human and mouse amino acid sequences. This allowed us to predict a virtual cDNA sequence of 932 bp, with five exons of similar sizes and conserved consensus splice acceptor and donor sequences, as for the human and mouse orthologous genes (fig. 3*a;* table 4), and encoding a putative polypeptide of 304 amino acids (fig. 4*a*). As expected, the genomic locus of *Fugu Nipa1* is much smaller than that of mammalian *NIPA1* loci and spans only ∼1.4 kb, not including the UTRs.

Characterization of the NIPA2 *Gene*

As with *NIPA1,* the human *NIPA2* gene was identified by *in silico* methods using BLAST of BAC 26F2 genomic sequence, as well as identification of a second CpG island in this BAC that represents the 5′ end of *NIPA2.* We compiled a synthetic *NIPA2* cDNA sequence of 2,450 bp, with an AATAAA poly(A) signal at positions 2444–2449 utilized for polyadenylation (fig. 3*c*). *NIPA2* spans 29 kb in the human genome and has seven exons (fig. 3*c*), each with consensus exon-intron boundaries (table 4), and for which exons 3–7 encode a NIPA2 putative polypeptide of 360 amino acids (fig. 4*b*). The mouse *Nipa2* cDNA (see the "Material and Methods" section) is very similar to human *NIPA2,* having seven conserved exons (fig. 3*c;* table 4), encoding a putative polypeptide of 359 amino acids in exons 3–7 (fig. 4*b*), and with this locus spanning 29.8 kb in the mouse genome. Two forms of the mouse *Nipa2* cDNA (1,867 bp and 3,200 bp; fig. 3*c*) differ in the positions of alternative polyadenylation sites in the 3′ UTR, created through the use of poly(A) signals at cDNA positions 1846–1851 (ATTAAA) and 3131–3136 (AATAAA). Both transcripts are observed in different tissues (see below).

We also sequenced and assembled a 1,805-bp *Gallus gallus Nipa2* cDNA, encoding a 361–amino acid putative polypeptide. Adjacent to the *Fugu Nipa1* gene, we identified the *Fugu Nipa2* ortholog, encoding a 366–amino acid putative polypeptide. There are five coding exons that correspond to exons 3–7 of the orthologous human and mouse genes (fig. 3*c*) with conserved exon-intron boundaries (table 4), although putative noncoding exons 1 and 2 have yet to be identified in *Fugu.* The *Fugu Nipa1* and *Nipa2* genes were found in conserved positions with respect to the mouse locus (fig. 1*f*), and *Fugu* orthologs for the *p, Herc2, Cyfip1,* and *Gcp5* genes were also identified in conserved positions (data not shown), providing strong evidence that each represents the ortholog of the mammalian genes. Finally, the position of the splice donor and acceptor sequences for the

fourth intron of *NIPA2* is conserved in all homologs analyzed (fig. 3*c*), including the single intron present in the insect "ancestral" gene, intron 2 for the "ancestral" *C. elegans* gene (total of six exons), and intron 2 of an *Arabidopsis* paralog with nine total exons.

Comparison of human *NIPA2* and mouse *Nipa2* cDNAs demonstrates two peaks of homology, one that begins at the NIPA2 start codon in exon 3 and the other that is a short region (∼120 bp) in exon 1 (fig. 3*d*). The latter encodes a potential 36-to-40–amino acid upstream ORF (uORF) that is conserved in mammals (figs. 3*d* and 3*e*), and several additional uORFs occur in exons 1–3. Distantly related uORF sequences also occur in the *NIPA2* 5′ region in chicken (where it is the second uORF) and *Xenopus* (fig. 3*e*). A conserved uORF, such as that observed here in *NIPA2* loci, is likely to regulate NIPA2 translation (Morris and Geballe 2000).

Polypeptide and Phylogenetic Analyses of the NIPA1 and NIPA2 Family

Analysis of the human, mouse, chicken, *Xenopus,* and *Fugu* NIPA1 and NIPA2 polypeptide sequences (figs. 4*a* and 4*b*), as well as the ancestral invertebrate and related plant members (fig. 4*b*), identified nine hydrophobic segments in each that likely encode putative transmembrane helices (TMH) (fig. 4*c*). Although the TMHMM program assigned a lower probability for TMH6 in human and mouse NIPA1, it is nevertheless clear that there is a hydrophobic domain of sufficient length to span the lipid bilayer and that TMH6 is clearly predicted in *Fugu* NIPA1, as well as in all related proteins (fig. 4*c*). We conclude that the *NIPA1* and *NIPA2* gene family encode polypeptides that have nine transmembrane-spanning helices.

Alignment of amino acid sequences of the NIPA1 polypeptide from human, mouse, and *Fugu* reveals these to be highly conserved (fig. 4*a;* table 5). Indeed, the human and mouse sequences display 98% identity, with a single amino acid change other than the length of the polyalanine tract, whereas NIPA1 in *Fugu* is ∼55% identical to that in mammals. Alignment of amino acid sequences of the NIPA2 polypeptide from human, mouse, chicken, *Xenopus,* and *Fugu* shows identities ranging between 78% and 96%, with the C-terminus being the most divergent (fig. 4*b;* table 5). Remarkably, NIPA1 and NIPA2 polypeptide sequences are related, with 32%–36% identity (and 47%–50% similarity) between any paralogous pair within these five species. Similarly, the ancestral *Drosophila, C. elegans,* and *Anopheles* polypeptides and a representative *Arabidopsis* member are highly related, with 40%–49% identity to vertebrate NIPA2 and lower identity (29%–34%) to vertebrate NIPA1 (table 5). The phylogenetic relationships are best seen in a tree diagram, which clearly illustrates the grouping of NIPA2 and NIPA1 homologs within vertebrates, and the distant ancestral members in invertebrates and *Arabidopsis*. The phylogenetic distance between NIPA1 and NIPA2 paralogs is as great as that between them and ancestral members, strongly suggesting that NIPA1 and NIPA2 have evolved related but different functions.

Analyses of Imprinting for BP1–BP2 Genes and Mouse Orthologs

The most proximal known imprinted gene in 15q is *MKRN3,* which is located just distal to BP2, although the presence of replication asynchrony in the pericentromeric region (see the "Introduction") and at mouse *Nipa1-Nipa2-Cyfip1* (fig. 2*c*) raises the possibility that the imprinted domain could extend further. Consequently, we tested whether the four BP1–BP2 region genes might be imprinted in human, using RNA from cells from patients with imprinting mutations who have two maternally (PWS) or two paternally (AS) imprinted chromosomes 15 (Buiting et al. 1995; Saitoh et al. 1996), as well as a somatic cell hybrid imprinting assay in which the rodent cell lines retain either a maternal or a paternal human chromosome 15 (Gabriel et al. 1998). RT-PCR shows that human *NIPA1* (both the major mRNA detected by a 167-bp band and a larger form with the alternatively spliced exon 3b), *NIPA2, GCP5,* and *CYFIP1* are each expressed in lymphocyte cells from a normal individual and PWS and AS imprinting mutation patients (figs. 5*a* and 5*b*), whereas *SNURF-SNRPN,* a paternally expressed imprinted gene in the PWS region as a control is only expressed in the normal and AS individuals (fig. 5*a*). In addition, *CYFIP1* is expressed from both the maternal and paternal chromosome 15 in somatic cell hybrids (fig. 5*b*). Therefore, the four BP1–BP2 genes are nonimprinted in peripheral blood lymphocytes and in fibroblasts.

To test imprinting in the mouse, we used a transgenic PWS and AS mouse model that has a paternally or maternally derived chromosome 7C deletion, respectively, spanning at least from *Frat3* through *Herc2* (Gabriel et al. 1999; Chai et al. 2001). On the basis of the deletion of BAC 252P22 (fig. 2*b*), the 3′ UTR of *Cyfip1* and all of *Nipa1* and *Nipa2* are included in the deletion (see fig. 1*f*), as are 5′ *Cyfip1* and *Gcp5* (J.M.G., J-H.C., and R.D.N., unpublished data), allowing this model to be used to test imprinting of these genes. All four genes (*Nipa1, Nipa2, Cyfip1,* and *Gcp5*) are expressed in wild-type, Tg$^{PWS(del)}$, and Tg$^{AS(del)}$ mice, resembling the control *Mkrn1* profile (fig. 5*c*). In contrast, the imprinted *Snurf-Snrpn* gene is not expressed in the PWS mouse, as expected (fig. 5*c*). Therefore, mouse *Nipa1, Nipa2, Cyfip1,* and *Gcp5* genes are expressed from both the paternal and maternal alleles and are nonimprinted in the brain.
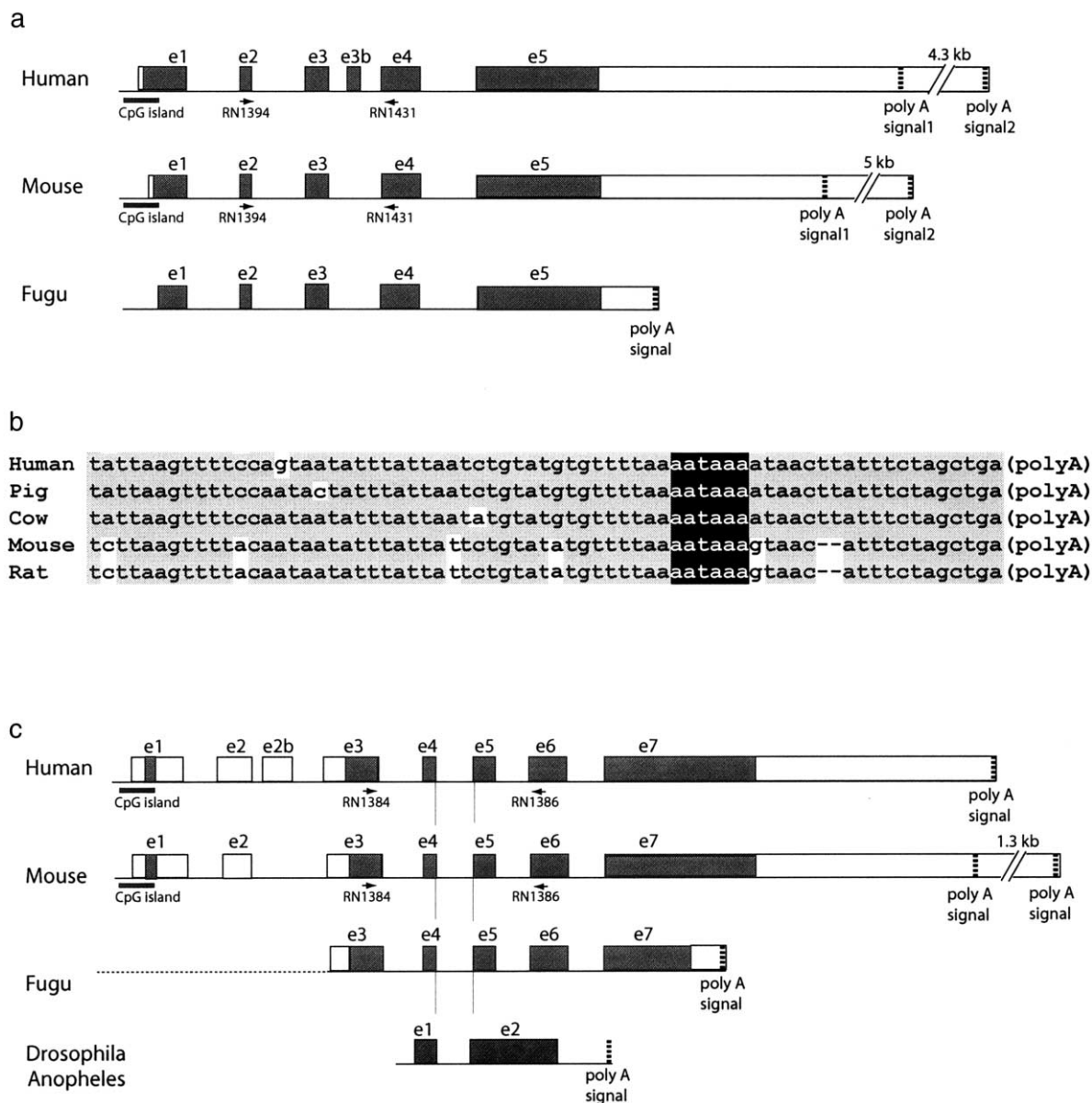
Figure 3 Vertebrate *Nipa1* and *Nipa2* gene structures. *a,* Schematic genomic structure of *NIPA1* in human, mouse and *Fugu*. Coding regions (*shaded rectangles*) and untranslated (5′ UTR and 3′ UTR) regions (*open rectangles*) are shown. The horizontal black bars are CpG islands, the arrows below the exons (e) are primers used for RT-PCR, and the vertical dotted lines are functional polyA signals (predicted in *Fugu*). Alternative polyadenylation generates two different 3′ ends for human and mouse *Nipa1* (with distance between the polyA signals shown). *b,* Highly conserved 3′ ends of the mammalian *NIPA1* 7.5-kb mRNA sequences from five eutherian species, aligned by CLUSTAL W. Black nucleotides with gray background agree with the consensus, and polyA signals are shown as white letters on black background. GenBank accession numbers for the *NIPA1* 3′ ESTs are as follows: human, BF439642; pig, BI339387; cow, BE685351; mouse, BE946294; and rat, AW533027. *c,* Genomic structure of orthologous human, mouse, and *Fugu NIPA2* genes, as well as conserved intron placement in ancestral genes from *Drosophila* and *Anopheles*. Symbols as for panel *a*. The shaded box in exon 1 represents uORF1, but putative 5′ noncoding exons in *Fugu* (*dotted line*) have not been identified. *d,* Conserved ORFs in the 5′ UTR (exons 1–3) of the vertebrate *NIPA2* transcripts. White letters on black background represent sequences conserved in all species shown, black letters with gray background have one mismatch, and the initiation codons of *NIPA2* and uORF1 have bold white letters on black background. Also shown are exon (ex) positions for the mouse (mu) gene, and the stop (TGA or TAA) codons for the uORF1. GenBank accession numbers for the *NIPA2* 5′ ESTs are as for fig. 4*b,*, and the GenBank accession number for dog is BM538411. Alignments were generated with CLUSTAL W. *e,* Amino acid sequence of the putative exon 1 uORF1 from human, mouse, cow, dog, chicken (uORF2), and *Xenopus NIPA2* mRNAs. White letters on black background represent sequences conserved by comparison with the mammalian consensus, and black letters with gray background represent sequences conserved in fewer species, and italics represent chemically similar amino acids. GenBank accession numbers are as for fig. 4*b,*and the GenBank accession number for chicken is AJ452290.

d

```
            CTAGGTCCCGGCAGCGGTGGTGACGGCGGTGCCGGAGGTTGTCCTTGGCAGGTTTTCCTC  60
human2
mouse2      ------------GGTGCTGGCCGCGGTGCGGCCGAAGGCTGTCCGAGGTAGGCTCCTCTC  48
dog2        --------------------------------------GCACGAGGGGCAGGTTCCCCTG  22

                    start uORF1
human2      GGCGCTTCTCCATGGAGGAGGCGGTGCCGAACGGCTTCAGCCCCGAATGCTCGCATCTCCC 120
mouse2      GGC--TCTCCATGGAGGAGGCGGCGCTCACTGC---AGTCTCGGATGCACGAACTTCCC  103
dog2        GGCGCTCCCCCATGGAGGAGGCGGCGGCGCGCGGGCTGCAGCCCCGAATGCTCTCGCTTCTT  82

human2      ACTGGACGGCGACGAAGGCGGTGGCCGTGCGAGCGCAGGA---------CTGGGCGGCCT 171
mouse2      GCGGGACGTCGCCGGAGACGGTGGCTGTGTGCGCGCAGGA---------GCGAGCTGCCT 154
dog2        TCTGTACGGCGACGAAGGCCCTGGCCGCGCGAGCTCGAGAGGCGGCGGCCCGTGCGGCCT 142

                    stop uORF1
human2      GTGTGGGCGGTGTGAGCGCCGGTGCCCAAGGCTGCGCCGCGAGGGGAAGCCGCGCGGCCG 180
mouse2      GCGTGGGCGGTCTGAGC---GGGCACCGGGGTCGCGTC--CCGGAGGGAGCCGAGTCGCCC 209
dog2        GTGTGGGCGTGTAAGCGGAGCTGACGAGGCCAGGGAGTGGAGAGCGCAGCCGCATGGCCG 202

                        start ex2(mu)
human2      GCCGGCCGAC--------TAGGGCTGGACGCTACTCGGCCCAGGGGTTAAGACTTTAAATGA 232
mouse2      GCCGGCCTGCGACGGCCCTAAGGGTGGAACTACTCTGCCGTGGTTAAATACTTTAAATGG 269
chicken2    ------------GAAACCTACCATTGGAAGTATTTAAGAAGCGAATGCCTCTGGATTTTG  46
dog2        GCCA-CCGCCCGGG----------------------------------------------- 215

human2      GAATAAAGGGTGGTATTTACGAGGAAATGAGAGTGAATAAGTCATCTCTAACCTCTCCCA 352
mouse2      GAATAAAGGATAGCGTTTCCAAGAAATGAGAATGAATAAATCATCTCTG---------- 319
chicken2    GAACAAATTGTGA-GTTTATGTGGAAGAGATGCTG--TGGCTGTTCTGAA---------- 95
dog2        ------------------------------------------------------------

                            start ex3 (mu)
human2      GCCTTTTTTCATAAGAGAGTCCATATTAAACTTACATGTTTGAAGACTGCTTCATTCTG 412
mouse2      -----TTTTTAAAGAAAGACCATATTAAACTTACATGTTTGAGGATTGCGTCACCTTG 374
chicken2    ------GCTCTGTGACAAA--------CTAACTTCAATGTTTCAGTATTGCATCACCTTG 129
dog2        --------------------------------------ATTTGAAGATTACATAGTCCTG 237

human2      CCTCTAGTACCAGCGGTTTCTCTGTTCTGTGATCAATGTGATTCACAGGAACTCCTTAAC 472
mouse2      TCTCCTGTACAAGCAGTTTCTCTGTTCGGTGATCAATGTCACTCACAGAACT---TAAGG 431
chicken2    TGTTGAGTAACAGGAGCTCTACTGTTCATTGATCAATGTG----ACAGTCCCC-----AG 182
dog2        CCTCCAGCACTAGTGCCTTCTCTGTTTTGTGCTCAATGTGACTCACAAGAACTTCTTTAC 297

                    Nipa2 start codon
human2      TAACAAACGAAATGAGCCAGGGGCGTGGAAAATATGA 509
mouse2      TAACTAACGAAATGAGCCTGGGGCGTGGAAAATATGA 468
chicken2    CAGTTTACGAGATGAGCCAAGCCCGTGGGAGATATGA 228
dog2        TAACAAACGAAATGATCCAGGGGCGTGGAAAATATGA 334
```

e

```
Dog          MEEAARAAAAPNALASFCTATKALAARAREAAARAACVGV*
Cow          MEEAVRTAAALDAHTSHWTETKAVAARAQEWVAGAACVGV*
Human        MEEAVRTASAPNARISHWTATKAVAVRAQDW---AACVGV*
Mouse        MEEAALTA-VSDARTSRGTSPETVAVCAQER---AACVGV*
Xenopus      MAEHRHSDEVSDPHLKSVD----ESEEKGINVGPTQA*
ChickuORF2   MELNRNLPLEVFKKRMPLDFGTNCEFMWKRCCGCSQAL*
```

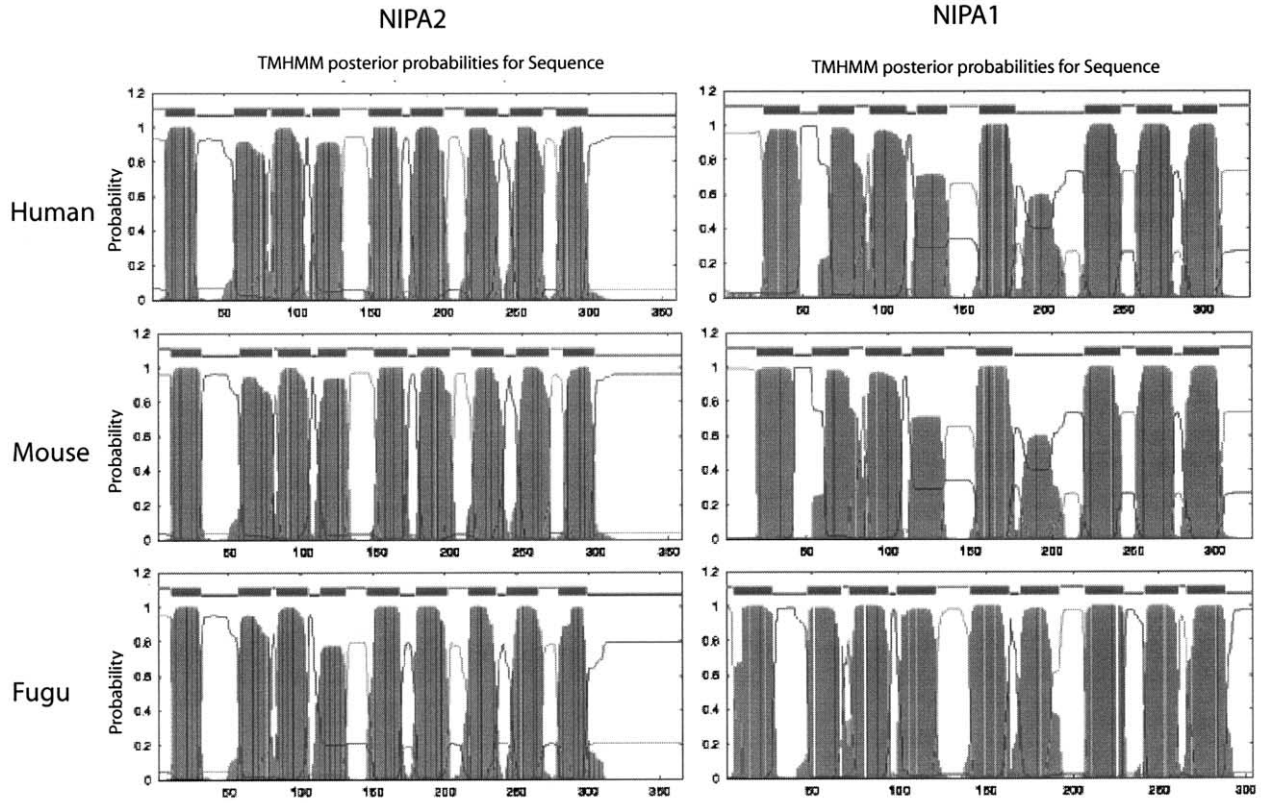*Expression Analyses of BP1–BP2 Genes and Mouse Orthologs*

The tissue patterns of expression for the four BP1–BP2 region genes and their mouse orthologs were studied by northern blot analysis. As predicted from cDNA and genomic analyses (see above), a single 2.4-kb transcript is seen for human *NIPA2* (fig. 6a), whereas 1.9 kb and 3.2 kb transcripts occur for mouse *Nipa2* (fig. 6b), with constitutive expression in both species including pronounced expression in the placenta (figs. 6a and 6b). In mouse, a 1.9-kb *Nipa1* transcript is also constitutive but at relatively low levels, whereas a larger (7.5-kb) mRNA is seen in several tissues, with both mRNA isoforms enriched in brain (fig. 6b). Similarly, the human *NIPA1* locus expresses a short (2.2-kb) and a long (7.5-kb) mRNA at low levels, with enrichment of the larger isoform in neuronal tissues (Rainier et al. 2003 [in this issue]). Similar studies with *CYFIP1* demonstrate a 4.4-kb constitutively expressed mRNA in human (fig. 6c) and mouse (fig. 6d), with highest levels in placenta (figs.
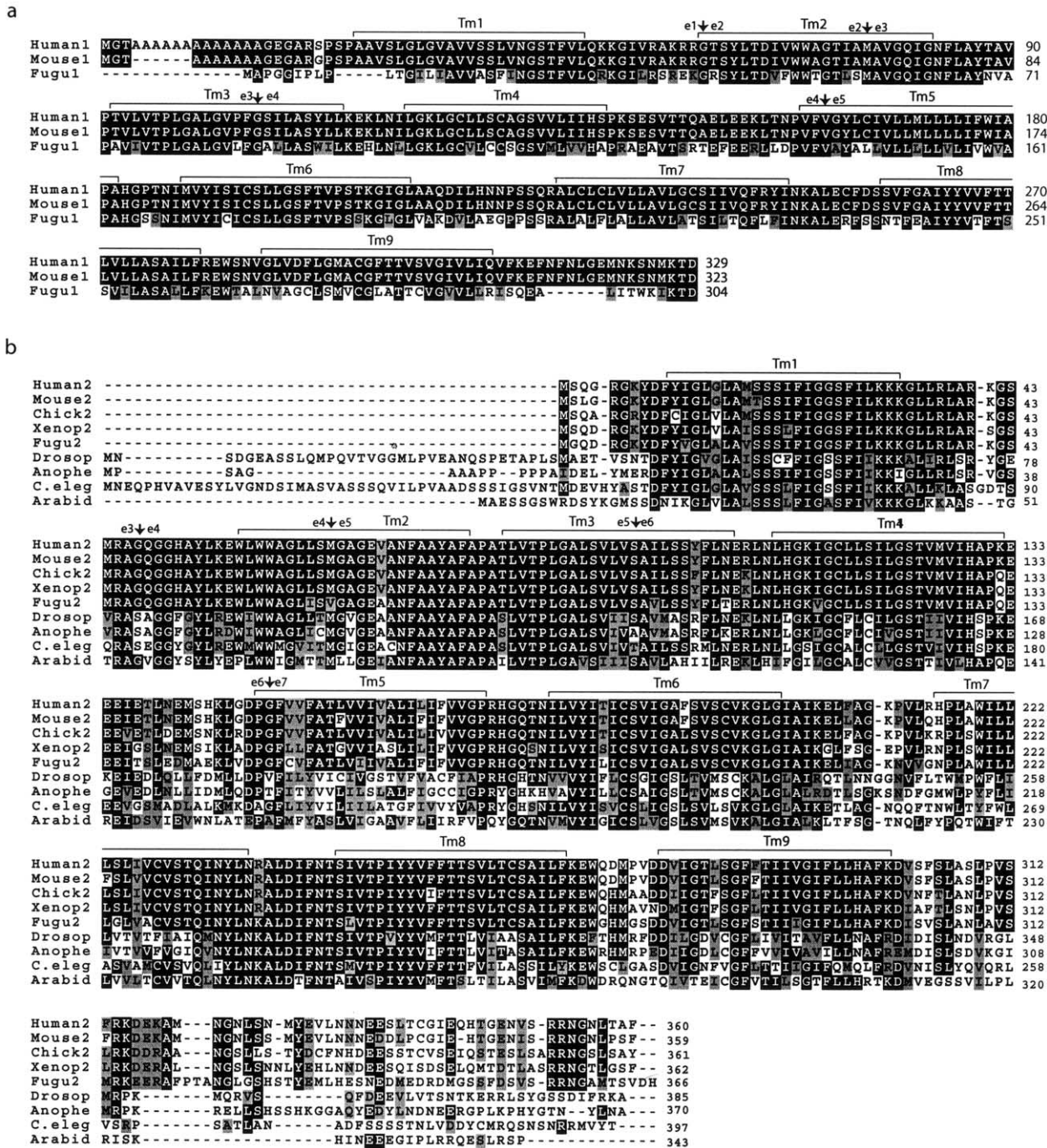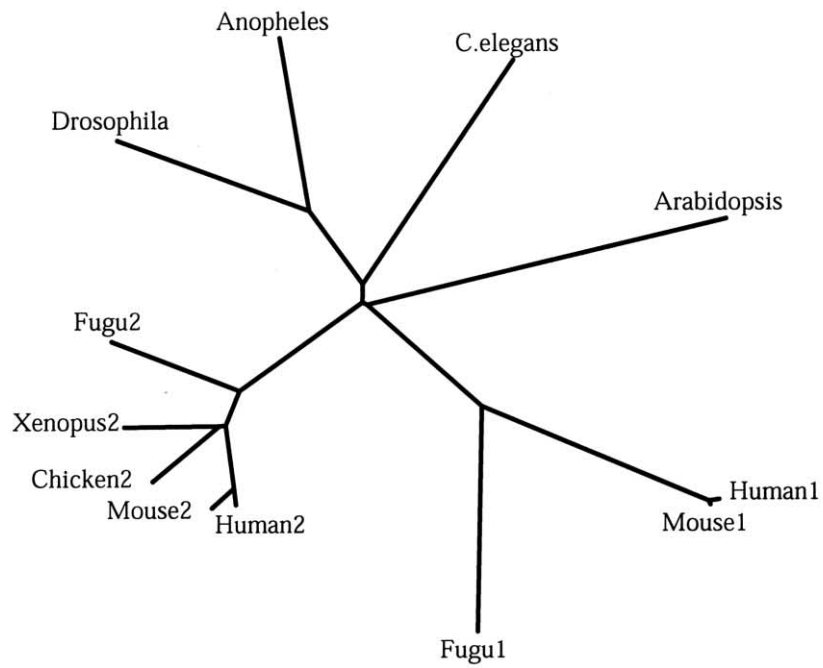
Figure 4   NIPA1 and NIPA2 polypeptides. *a,* Amino acid alignment of NIPA1 orthologs in human, mouse, and *Fugu*. White letters with black background represent identical residues, black letters with light gray shading indicate conserved substitutions. Putative transmembrane (Tm) domains are designated by brackets, and the positions of exon (e)-intron boundaries are shown. GenBank accession numbers are: human NIPA1, BK001020; mouse Nipa1, AY098645; and *Fugu* Nipa1 was predicted from genomic sequence (see the "Material and Methods" section). *c,* Amino acid alignment of NIPA2 orthologs from human (GenBank accession number BK001120), mouse (GenBank accession number BK001121), chicken (GenBank accession number AY099502), *Xenopus* (GenBank accession number BK001125), *Fugu* (predicted as for panel *a*), ancestral genes from *Drosophila* (GenBank accession number AE003637), *Anopheles* (predicted from GenBank accession number AAAB01008980), *C. elegans* (GenBank accession number AC006804), and a representative *Arabidopsis* homolog (GenBank accession number AY046035). Symbols as for panel *a*. *c,* Representative transmembrane helices based on hydrophobicity plots. *d,* Phylogenetic comparison of vertebrate NIPA1 and NIPA2 orthologs, ancestral invertebrate homologs and a representative *Arabidopsis* homolog. The tree was constructed using CLUSTAL W, and branch lengths are proportional to sequence divergence. Each polypeptide is designated as the species, and the number 1 or 2 designates NIPA1 or NIPA2, respectively, except for ancestral members.

c

NIPA2

NIPA1

TMHMM posterior probabilities for Sequence

TMHMM posterior probabilities for Sequence

Human

Mouse

Fugu

d

Anopheles

C.elegans

Drosophila

Arabidopsis

Fugu2

Xenopus2

Chicken2

Mouse2

Human2

Human1

Mouse1

Fugu1

913

Table 4

Exon-Intron Structures of *NIPA1* and *NIPA2* in Human, Mouse, and *Fugu*

Gene, Exon, and Species	cDNA Position (bp)	Splice Acceptor Intron Exon	Exon Size (bp)	Splice Donor Exon Intron[a]
NIPA1:				
1[b]:				
Human	1	5′ UTR + AUG codon	203	AAGCGGCGAGgtagggcgggcg
Mouse	1	5′ UTR + AUG codon	165	AAAAGGCGAGgtagggcgggcc
Fugu	1	5′ UTR + AUG codon	121	CGTGAAAAAGgtagagcacata
2:				
Human	204	ctcattttttataagGTACTTCCTA	48	ACAATCGCAAgtaagtagcctg
Mouse	166	caccttttttatagGTACTTCCTA	48	ACAATTGCAAgtaagtggttta
Fugu	122	atgtgttttccacagGACGTTCGTA	48	ACGTTGTCCAgtgagtacaggg
3:				
Human	252	tgattttcttgacagTGGCTGTTGG	91	TACCGTTCGGgtgagagccaag
Mouse	214	tgattctcttgacagTGGCTGTCGG	91	TACCGTTTGGgtgagaactgac
Fugu	170	ctgtgcataaaacagTGGCTGTAGG	91	TCCTATTTGGgtaggtcttaga
3b:				
Human[c]	NA	tctgctgtattccagACAGATGCCC	82	AGGCATTAAGgttctgtgacct
4:				
Human	343	ctttttttcaataaagGTCCATTTTA	161	ACCAACCCAGgtaattcctttc
Mouse	305	tttccttaattgaagGTCCATTTTA	161	ACCAATCCAGgtaactcgttct
Fugu	261	gttgttgacacgcagAGCTCTGCTG	161	CTGGACCCAGgtcagtttgttt
5:				
Human	504	ctgtctgtgttccagTGTTTGTGGG	1,744[d]	Stop codon + 3′ UTR
Mouse	466	ccatctgtcttgcagTGTTTGTGGG	1,419[d]	Stop codon + 3′ UTR
Fugu	422	ttttccaccctgcagTGTTTGTGGC	>511[d]	Stop codon
NIPA2:				
1[e]:				
Human	1	5′ UTR	245	GCCGACTAGGgtgaggtcgcca
Mouse	1	5′ UTR	231	CGGCCCTAAGgtagctacttcc
Fugu	Unknown			
2[d]:				
Human	246	ttttcttctttctagGCTGGAGCTA	136	AAACTTACATgtaagttaaaat
Mouse	232	ttttcttctttccagGGTGGAACTA	121	AAACTTACATgtaagttaaaat
Fugu	Unknown			
2b[c]:				
Human	NA	atatctctgttgcagGCTCTCCCGG	122	ATTTTCAAACgtaagtcagaatg
3[b]:				
Human	382	ttttttattgtttagGTTTGAAGAC	232	ATGAGAGCAGgtaggttatgcc
Mouse	353	ttttatatcatttagGTTTGAGGAT	229	ATGAGAGCAGgtaagttatgtc
Fugu	1	AUG codon	139	ATGCGGGCAGgtattcaaccct
4:				
Human	614	tttcttcattcacagGTCAAGGTGG	57	CTGCTGTCAAgtatgtataaag
Mouse	582	aatatttcttcacagGTCAAGGAGG	57	CTGCTGTCAAgtatgtatagag
Fugu	140	gttccctcccttcagGCCAGGGCGG	57	CTGCTGTCAAgtaagtctaatt
5:				
Human	671	ttgtctgtctctaagTGGGAGCTGG	91	TGCTAGTAAGgtaaggacacgt
Mouse	639	tgttcatctcttcagTGGGAGCCGG	91	TCCTCGTAAGgtaagactctgt
Fugu	198	tatttgtctttacagTGGGGGCGGG	91	TGCTCGTCAGgtactctgctca
6:				
Human	762	tcctccccattttagTGCCATTCTT	161	GGTGATCCAGgtaagaaaaaag
Mouse	730	tattcttcctttttagTGCCATTCTG	161	GGTGATCCAGgtaagaaaaaac
Fugu	290	taaatgtcactgcagTGCTGTGCTG	161	GTGGATCCAGgtagcgagcggc
7:				
Human	923	ctttgcctcctccagGTTTTGTGGT	1,506[d]	Stop codon + 3′ UTR
Mouse	881	ctttgcttcctctagGTTTTGTGGT	977[d]	Stop codon + 3′ UTR
Fugu	451	ccgtcttctctccagGGTTTTGTGT	>357[d]	Stop codon

[a] Lowercase letters refer to intron sequences, and uppercase letters refer to exon sequences. Underlined letters "ag" and "gt" represent consensus splice acceptor and donor sequences, respectively.

[b] Exon encoding AUG start codon.

[c] Low level alternatively spliced exon; NA = not applicable.

[d] First polyA signal (human, mouse) or stop codon (*Fugu*).

[e] Noncoding 5′ exon (may encode uORF).

Table 5

Phylogenetic Comparison of NIPA2 and NIPA1 Orthologs/Paralogs

	Human 2	Mouse 2	Chicken 2	Xenopus 2	Fugu 2	Anopheles	Drosophila	C. elegans	Arabidopsis	Human 1	Mouse 1	Fugu 1
					PERCENT IDENTITY AND PERCENT SIMILARITY[a]							
Human 2	100	96	86	83	78	48	44	45	42	35	36	34
Mouse 2	97	100	83	81	77	48	43	44	40	35	36	33
Chicken 2	90	87	100	84	75	47	44	45	43	35	35	34
Xenopus 2	88	87	90	100	75	46	44	45	43	34	35	33
Fugu 2	84	84	84	82	100	47	42	44	41	33	34	33
Anopheles	62	61	61	60	62	100	62	48	39	32	31	29
Drosophila	58	58	58	58	57	74	100	46	40	34	33	31
C. elegans	58	57	60	60	57	63	60	100	38	32	32	29
Arabidopsis	56	55	58	57	55	54	54	53	100	30	31	32
Human 1	50	49	49	48	48	47	49	48	45	100	98	55
Mouse 1	50	50	50	48	49	47	48	47	46	98	100	56
Fugu 1	48	48	47	46	47	43	44	43	47	69	70	100

[a] In each column, the numbers above those that are underlined indicate identity, and the numbers below those that are underlined indicate similarity.
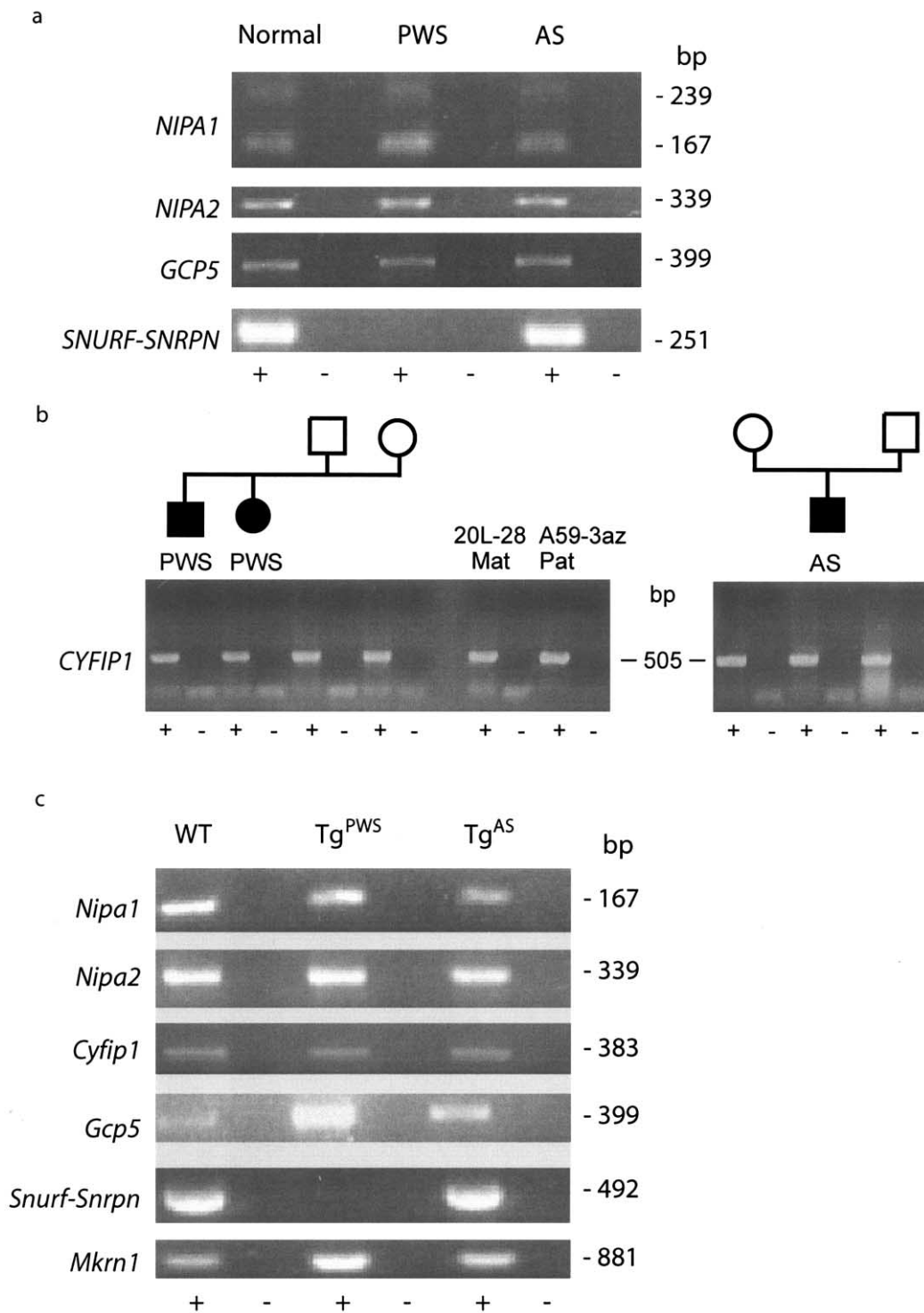
Figure 5 Imprinting assay of BP1–BP2 genes by RT-PCR in human and mouse. *a, NIPA1, NIPA2,* and *GCP5* mRNA expression was examined in lymphoblast cell lines derived from a normal individual and from patients who have PWS (PWS-U) and AS (AS-J) with imprinting defects. An imprinted control gene, *SNURF-SNRPN,* shows paternal-only expression, as detected in the AS but not the PWS cell line. + = RT present; − = RT minus control. *b, CYFIP1* imprinting analysis in families PWS-U and AS-J with imprinting defects and in somatic cell hybrids with a single maternal (Mat) or paternal (Pat) human chromosome 15. *c, Nipa1, Nipa2, Cyfip1, Gcp5,* imprinted control *Snurf-Snrpn,* and control *Mkrn1* mRNA expression in mouse. Brain mRNA from wild-type (WT), or transgenic-deletion mouse models of PWS (Tg[PWS]) and AS (Tg[AS]) were used for RT-PCR. *Mkrn1* is a nonimprinted control gene from mouse chromosome 6A (Gray et al. 2000). Paired lanes show reactions with (+) or without (−) reverse transcriptase.
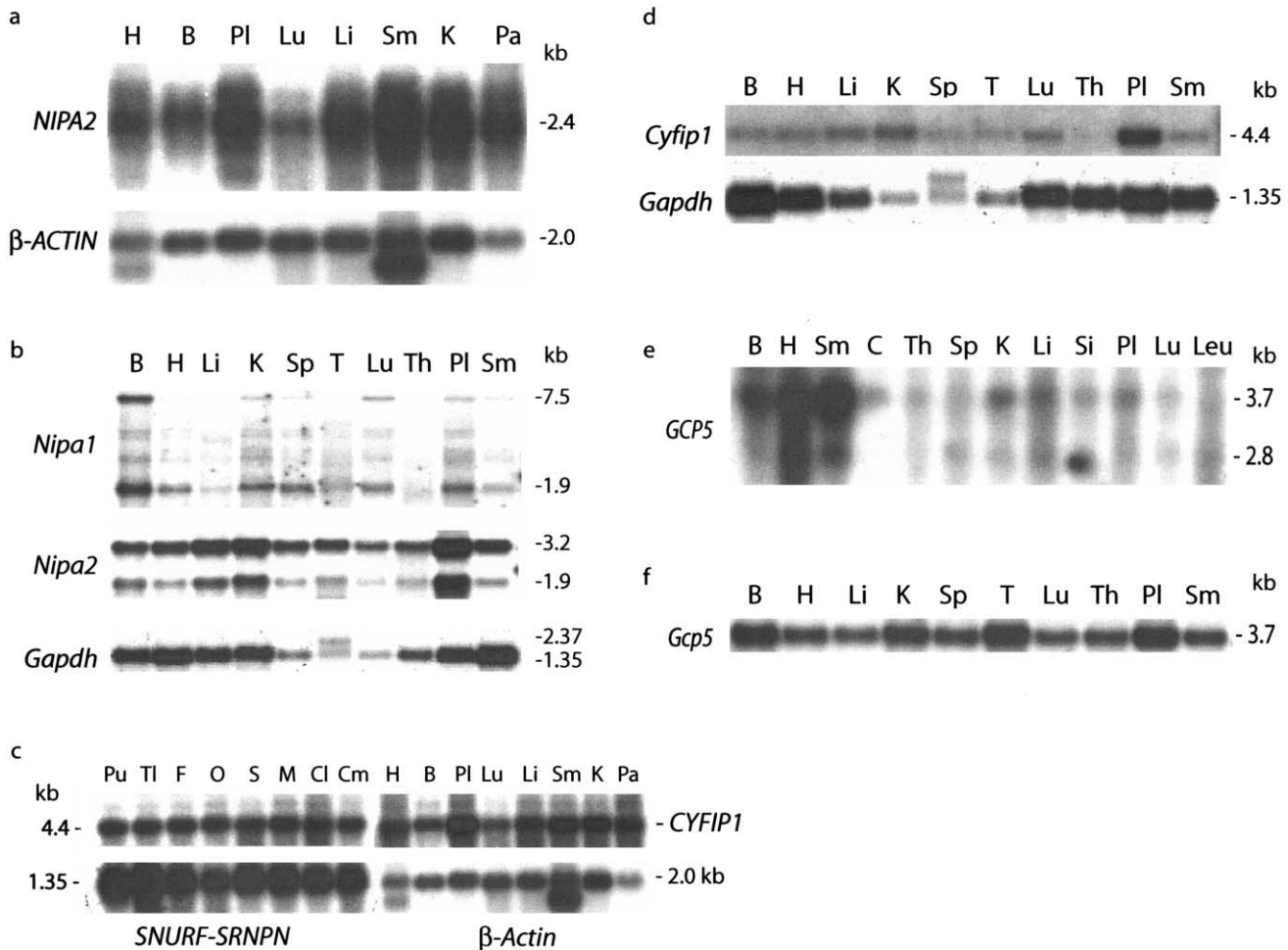
Figure 6 Expression of BP1–BP2 genes in human and mouse tissues. *a,* Expression of human *NIPA2* in various tissues by northern analysis, with *β-ACTIN* as a control. *b,* Constitutive expression of *Nipa2* and brain-enriched expression of *Nipa1* in mouse tissues by northern blot analysis, with *Gapdh* as a control. *c,* Expression of *CYFIP1* in different human tissues and regions of brain, with *SNURF-SNRPN* or *β-ACTIN* as controls. *d,* Mouse *Cyfip1* is widely expressed and enriched in placenta. *Gapdh* expression serves as a control. *e,* Human *GCP5* is expressed at high levels in muscle and at lower levels in other tissues. *f,* Mouse *Gcp5* is constitutively expressed in different tissues. In each case, radioactivity from each blot was stripped prior to successive hybridizations. B = brain; C = colon; Cl = cerebral cortex; Cm = cerebellum; F = frontal lobe; H = heart; K = kidney; Leu = peripheral blood leukocyte; Li = liver; Lu = lung; M = medulla; O = occipital lobe; Pa = pancreas; Pl = placenta; Pu = putamen; S = spinal cord; Si = small intestine; Sm = skeletal muscle; Sp; spleen; T = testis; Th = thymus; and Tl = temporal lobe.

6c and 6d) and equal levels throughout the brain (fig. 6c). *GCP5* has a 3.7-kb transcript in human (fig. 6e) and mouse (fig. 6f), with the former enriched in muscle tissues, whereas a smaller (2.8-kb) *GCP5* mRNA is also seen in some tissues. Mouse *Gcp5* is also enriched in placenta (fig. 6f), as is true for *NIPA2* and *CYFIP1* in human and mouse.

Discussion

Chromosome rearrangements involving BP1 or BP2 in 15q11.2 include proximal deletion end points for PWS/AS deletions (Amos-Landgraf et al. 1999; Christian et

al. 1999), duplications, and triplications (Roberts et al. 2002) and for inverted duplicated chromosomes (inv dup [15]) (Cheng et al. 1994; Leana-Cox et al. 1994; Huang et al. 1997). Numerous duplicons mapping to the BP1, BP2, and BP3 segments appear to be transcribed pseudogenes, including *HERC2* duplicons, a truncated copy of poly(A)-specific ribonuclease from 16p13, LCR15 duplicons that include the golgin-like protein gene and *SH3P18* also mapped at 15q24 and 15q26, and sequences encoding an ATP-binding cassette protein, a BEM-1/BUDS suppressor-like protein, and *MYLE* (Buiting et al. 1999; Amos-Landgraf et al. 1999; Christian et al. 1999; Ji et al. 1999; Pujana et al. 2001).

Similarly, only large duplicated and rearranged blocks of sequences derived from other chromosome locations have been mapped centromeric of BP1 (Ritchie et al. 1998; Fantes et al. 2002). Here, we have unequivocally demonstrated that four highly conserved genes (*NIPA1, NIPA2, CYFIP1,* and *GCP5*) are located in a genomic domain between BP1 and BP2. Our observations have significant implications for the delineation of the PWS imprinted domain; for understanding the basis of nonimprinted genetic diseases that map to this chromosomal region in human and the homologous chromosome region in mouse, including modification of the PWS or AS phenotype; and for an understanding of the fluidity of the genome during evolution and the way this mirrors events that occur mechanistically as de novo events in human disease.

Implications for Genomic Imprinting Mechanisms

All four genes between BP1 and BP2 in 15q11.2 were shown here to be nonimprinted in lymphoblastoid cell lines and human-rodent somatic cell hybrids, with the mouse orthologs nonimprinted in brain. The latter observation is important because most, if not all, the imprinted loci in the PWS/AS imprinted domain are predominantly expressed and imprinted in the brain (Nicholls and Knepper 2001). We conclude that the mammalian *NIPA1, NIPA2, CYFIP1,* and *GCP5* genes are nonimprinted. Although the four mouse genes map ∼2 Mb from the imprinted domain, the human orthologs are separated from the PWS imprinted domain solely by BP2 sequences; however, the size of BP2 is poorly defined because of the complex and incompletely known composition of duplicons. Since the *HERC2* duplicons within BP2 include the CpG-rich promoter and are derived from a nonimprinted locus (Amos-Landgraf et al. 1999; Ji et al. 1999), we suggest that one model to explain the proximal imprint boundary might simply be the evolutionary integration of "nonimprintable" promoter sequences adjacent to the imprinted domain. In contrast, when genes such as mammalian *MKRN3* and rodent *Frat3* were duplicated by retroposition, they had promoters that were subject to the imprint process when these genes integrated into or adjacent to the imprinted domain (Chai et al. 2001).

Several studies have shown replication asynchrony in domains with monoallelic gene expression, including those imprinted (Kitsberg et al. 1993; Chess et al. 1994; Knoll et al. 1994; Hollander et al. 1998; Simon et al. 1999; Mostoslavsky et al. 2001) and with a transition from imprinted to nonimprinted sequences at mouse *H19,* defined by an asynchronous to synchronous replication change (Greally et al. 1998). The use of marked mouse chromosomes 7 gave us an extremely useful tool for analysis of replication patterns at the *Nipa1-Nipa2-Cy-*

fip1 domain, where we found asynchrony that was random with respect to parental origin. A similar pattern has been described elsewhere for the *P* (*OCA2*) locus in human 15q13 (Knoll et al. 1994), whereas imprinted loci replicate the chromosome derived from one parent (usually the paternal allele) earlier than the other (Kitsberg et al. 1993; Knoll et al. 1994; Simon et al. 1999). The *OCA2* locus is ∼1.5–2 Mb from the imprinted domain, whereas the mouse region studied here is ∼2–2.5 Mb from the mouse 7C imprinted domain. It is possible that the transition from asynchrony determined by parent of origin to the pattern of random asynchrony that we have demonstrated here is detectable only with the use of a marked chromosome such as that used in this study. Our finding that the four genes in the BP1–BP2 region are nonimprinted suggests that the asynchronous DNA replication observed proximal to deletion breakpoint BP1 (Ritchie et al. 1998) may be another example of the same phenomenon and does not indicate a more extensive imprinted domain. Rather, replication asynchrony may identify those chromosomal regions with the capacity for monoallelic gene expression: however, we propose that other factors, including DNA methylation and/or elements of the histone code (Jenuwein and Allis 2001; Turner 2002), are mechanistically needed to complete the silencing or activation of individual alleles.

Functional Considerations of a New Gene Family

Two of the four genes identified in the BP1–BP2 region are the related *NIPA1* and *NIPA2* genes. Phylogenetic studies indicate that both paralogous gene members are ancient and likely arose 450–600 million years ago, around the time of the origin of vertebrates. Despite the adjacent chromosome linkage of *NIPA1* and *NIPA2* and retention of this syntenic relationship in all examined vertebrates, there is no evidence that one served as the precursor to the other. Indeed, four additional NIPA1/2-related paralogous family members are dispersed in vertebrate genomes, and each appears to have arisen early in vertebrate evolution (J-H.C. and R.D.N., unpublished data). Alternatively, *NIPA1* or other family members may be evolutionarily younger, and, after their origin, they may have gone through a period of rapid mutation, followed by fixation and a dramatic slowdown in mutation rate. Further study of this gene family in extant vertebrate species will shed light on the evolutionary history of this novel gene family.

NIPA1 and *NIPA2* differ in gene structure and expression patterns, reflecting their ancient origins; however, in both cases, there are five coding exons, and these show homology in intron placement. In particular, the only intron in the insect *NIPA1/2* gene is conserved in position in all vertebrate *NIPA2, NIPA1,* invertebrate, and plant family members, despite variation in exon

number. During evolution of *NIPA2*, two 5′ noncoding exons arose along with the coding potential for a small uORF. The presence of one or more uORFs in *NIPA2* suggests that this gene undergoes translational regulation (Morris and Geballe 2000) and that translation of *NIPA2* may involve an internal ribosome entry site mechanism (Fernandez et al. 2002), although further work will be necessary to examine these possibilities. In contrast to the constitutive expression of *NIPA2* and the smaller *NIPA1* transcript in all tissues of human and mouse, *NIPA1* shows high levels of brain-enriched expression of a 7.5-kb transcript (as shown here and in the article by Rainier et al. 2003 [in this issue]). The mechanism for this may reflect stabilization of the mRNA in brain for the long form of *NIPA1*, transcriptional activation plus coordinate polyA site selection in a neuron-specific manner, or silencing of the latter transcription-polyadenylation pattern in nonneural tissues, as occurs with the neuron-restrictive silencer factor (Zhao et al. 1999; Lunyak et al. 2002; Proudfoot et al. 2002; Worthington et al. 2002).

Our prediction of a nine-TMH helix domain structure for the NIPA1 and NIPA2 polypeptides suggests that they function as either receptors or transporters. NIPA1/2 show low homology, spanning three TM domains (∼29% over ∼93 amino acids), with some G-protein coupled receptors, such as extracellular calcium receptors and olfactory receptors (data not shown); however, this may reflect the hydrophobic nature of TM domains, and any functional or evolutionary relationship remains conjecture. Indeed, polypeptides with nine TM spanning passes of the lipid bilayer are rare. Exceptions are glucose-6-phosphatase (Pan et al. 1998), a cardiac $Na^{+/-}$-Ca^{2+} exchanger (Qiu et al. 2001), and the TM9 domain superfamily (TM9SF) (Chluba-de Tapia et al. 1997); TM9SF members are localized to endosomes (Schimmöller et al. 1998), bind the synthetic ligands cyanopindolol and the β-adrenergic agonist SM-11044, and have roles in colon relaxation and eosinophil chemotaxis (Sugasawa et al. 2001), or are involved in adhesion and phagocytosis in *Dictyostelium* (Cornillon et al. 2000). However, the TM9SF family is unrelated in primary sequence to the NIPA1/2-family. Furthermore, whereas TM9SF members have a signal peptide (type I topology), members of the NIPA1/2-family do not, and the latter must have internal membrane targeting sequences. Consequently, the function of the NIPA1/2 family remains unknown. Nevertheless, the presence of distinct family members in vertebrates, invertebrates, plants, and bacteria (the present article; J-H.C. and R.D.N., unpublished data) indicates that these conserved polypeptides are likely to be critical for signaling within or between cells. Studies with antibodies and with animal models deficient in or overexpressing these genes, as well as iden-

tification of ligands for these polypeptides, are now necessary to determine their functions.

Implications of BP1–BP2 Region Genes for Hereditary Disease

Since blocks of duplicated sequences that are implicated in homologous recombination flank the BP1–BP2 region genes, chromosome rearrangements involving the BP1–BP2 region may lead to dosage imbalance or rearrangements of the *NIPA1, NIPA2, CYFIP1,* and *GCP5* genes. This includes loss of one allele in the larger class I chromosome deletions in PWS and AS, or gain of one or two alleles, in 15q11-q13 duplications and triplications as well as for inv dup (15) marker chromosomes (Knoll et al. 1990; Cheng et al. 1994; Leana-Cox et al. 1994; Huang et al. 1997; Amos-Landgraf et al. 1999; Christian et al. 1999; Roberts et al. 2002). On the basis of the finding of small inv dup (15) marker chromosomes with the BP1–BP2 region but not the PWS/AS region in a series of patients with generally normal phenotypes, Huang et al. (1997) concluded that no genes in these small markers have clinically relevant dosage effects. In contrast, recent studies by Butler et al. (2003) found that PWS subjects with class I deletions (BP1–BP3) have a more severe phenotype than those with class II deletions (BP2–BP3), including greater self injurious behavior, deficits in adaptive behavior (including motor skills), obsessive-compulsive behavior, and difficulties with reading, mathematics skills, and visual-motor integration. These data provide evidence that deletions of the four genes in the BP1–BP2 region may be associated with dosage-sensitive behavioral and psychological phenotypes. We propose that some individuals may have a condition with just these types of clinical phenotypes and a deletion or duplication limited to the BP1–BP2 region due to recombination between duplicated sequences within BP1 and BP2. Further study of BP1–BP2 region genes and chromosome rearrangements will determine whether the presence of four highly conserved genes flanked by unstable DNA sequences can have a significant phenotypic impact.

A chromosome 15 rearrangement limited to the unique 250-kb BP1–BP2 region was recently found in a subject with PWS due to a 15q11-q13 deletion that arose on the paternally inherited chromosome containing a familial duplication limited to BP1–BP2 (Butler et al. 2002). Consequently, duplications, deletions, or inversions limited to the BP1–BP2 region may predispose to subsequent larger rearrangements of proximal 15q. Indeed, a polymorphic 1.5-Mb inversion within a similar class of duplicated sequences in chromosome 7q11.23 is associated with susceptibility to deletion of the 1.5-Mb region in Williams-Beuren syndrome (Osborne et al. 2001). Similarly, inversions of BP2–BP3 were identi-
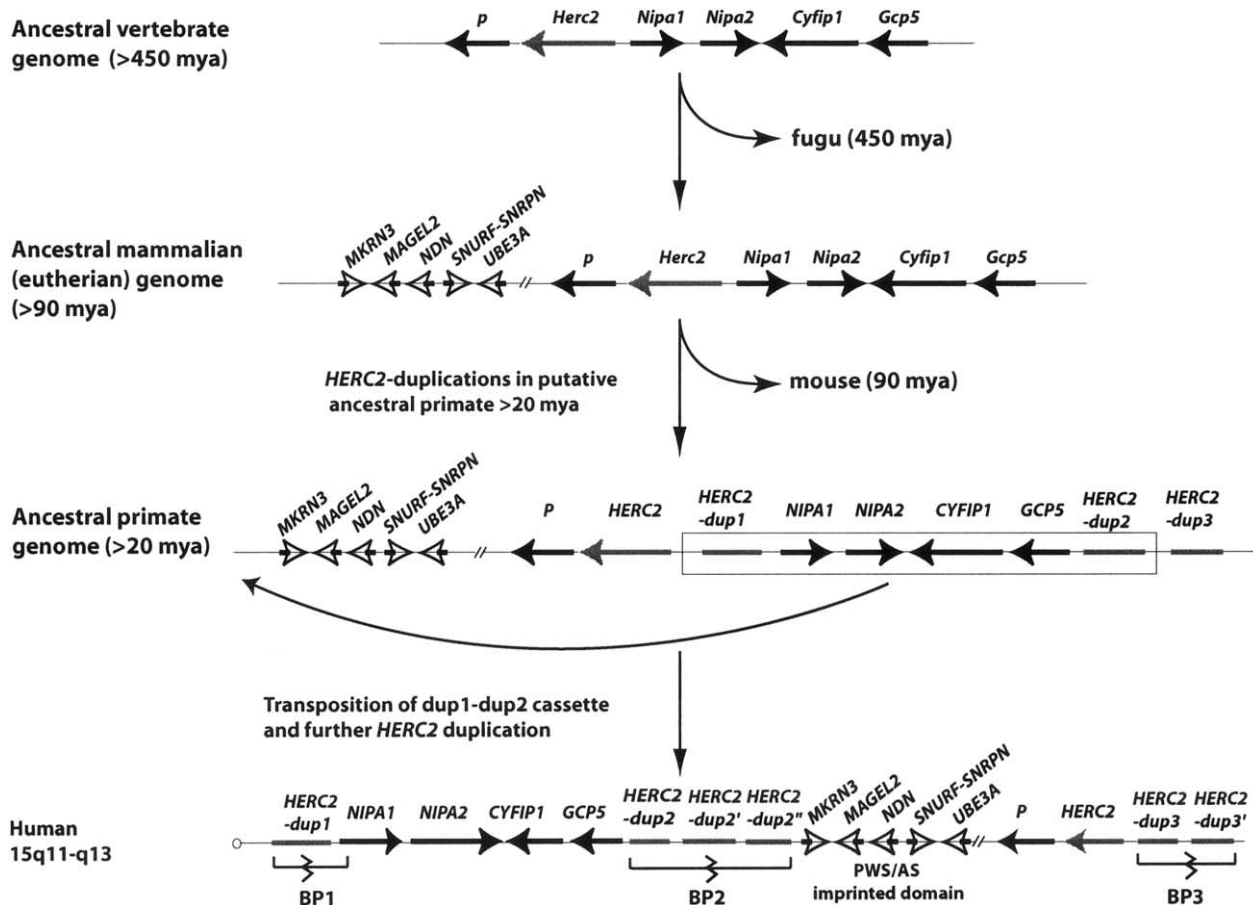
Figure 7 Model for evolutionary transposition of BP1–BP2 genes by flanking duplicons. Genes are shown as horizontal arrows or arrowheads indicating the direction of transcription. Black arrows and white arrowheads represent nonimprinted and imprinted genes, respectively. *HERC2* and duplicons (dup) derived from *HERC2* are shown as gray arrows or bars when transcriptional direction is unknown. The rectangle indicates a putative transposition of a four-gene cassette with flanking *HERC2*-duplicons, in an ancestral primate. See text for further details. Not shown in this schematic is a cluster of three GABA$_A$ receptor genes and *ATP10C*, located between the *UBE3A* and *P* loci in human and mouse, nor additional duplicons that are interspersed with *HERC2* duplicons but that are poorly characterized to date (see Nicholls and Knepper 2001).

fied in four of six mothers of patients with AS deletion (Gimelli et al. 2003), which supports the previous finding of a familial 15q11-q13 inversion in the mother and father of deletion patients with AS and PWS, respectively (Clayton-Smith et al. 1993), consistent with the large inversion being a predisposition allele. Indeed, BP1–BP2 deletions or other rearrangements may be more common than the PWS/AS deletions, which occur at an overall frequency of ~1/10,000 newborns, since the distance between the putative recombining segments is only a fraction of that of the 4–4.5-Mb PWS/AS deletions.

All four BP1–BP2 region genes are candidates for dominantly inherited spastic paraplegia, locus 6 (SPG6 [MIM 600363]). SPG6 is characterized by insidiously progressive lower-extremity spasticity in which axonal degeneration affects primarily the longest axons in the CNS and is caused by a mutation within a 7.3-cM seg-

ment spanning the PWS/AS region (Fink at al. 1995). The finding of obligate recombinants for markers within the cluster of GABA$_A$ receptor genes in distal 15q11-q13 ruled these out (Fink et al. 1996). As a dominant disorder, SPG6 is not expected to be associated with imprinted genes, ruling out most other genes in the PWS/AS deletion region. Since no functional genes are known proximal to BP1, the BP1–BP2 region genes, particularly *CYFIP1* and *GCP5*, became prime candidates. CYFIP1 associates with Rac1 and F-actin (Kobayashi et al. 1998), with Rac1 implicated in regulation of the actin cytoskeleton, including axon growth, guidance, and branching (Ng et al. 2002). CYFIP1 also associates with FMRP (Schenck et al. 2001), the fragile X mental retardation protein, which is implicated in neurite extension, guidance, and branching (Morales et al. 2002). In addition, *GCP5* encodes a protein that is part of the

human γ-tubulin complex required for microtubule nucleation at the centrosome (Murphy et al. 2001). Microtubules are critical in axonal transport, and defects in this process are known in spastic paraplegias (Crosby and Proukakis 2002). However, although *NIPA1* and *NIPA2* are of unknown function, the CNS-specific expression of *NIPA1* made it an attractive and correct candidate (Rainier et al. 2003 [in this issue]).

Mutation studies of the mouse orthologs of the four BP1–BP2 region genes will shed light on the potential phenotypic role of recessive loss-of-function mutations in these genes. Indeed, a locus required for embryo implantation, *l71Rl,* was identified just proximal to the pink-eyed dilution (*p*) gene on the basis of recessively inherited deletions of the region (Wu et al. 2000). Genetic complementation and molecular mapping define the critical interval for *l71Rl* as a small region between *D7Mit70* and *5′ Herc2* (Wu et al. 2000), to which we have mapped the mouse *Nipa1, Nipa2, Cyfip1,* and *Gcp5* genes, making one or more of these four genes likely candidates for *l71Rl*. Although the homologous human chromosome BP1–BP2 region is flanked by unstable DNA sequences, as discussed above, the mouse *l71Rl* data indicate that it is unlikely that individuals will exist who are homozygously deleted for the BP1–BP2 region, since such homozygous deletions would be predicted to be associated with a failure of the embryo to implant. Should BP1–BP2 deletions occur in association with a normal or mild neurobehavioral phenotype (see above), their inheritance from each parent might be associated with early pregnancy loss and thus may represent an important genetic counseling issue.

Evolutionary Transposition of BP1–BP2 Region Genes Mirrors Recombination Events in Genomic Disease

We have shown that a block of at least six genes (*OCA2, HERC2, NIPA1, NIPA2, CYFIP1,* and *GCP5*) are syntenic in human, mouse, and *Fugu;* however, in human, the latter four genes have transposed to a site ~4 Mb away from the OCA2 and *HERC2* genes. These and previously published data allow us to propose a model for the evolution of human 15q11-q13 (fig. 7). Mouse and *Fugu* are representative of the ancestral vertebrate arrangement of these genes (fig. 7). The evolutionarily young imprinted domain was subsequently added in mammals, adjacent to this ancestral domain (fig. 7) (Chai et al. 2001; Nicholls and Knepper 2001). During evolution of an ancestral primate, 25–60 million years ago (Amos-Landgraf et al. 1999; Christian et al. 1999; Ji et al. 1999; Locke et al. 2001), the *HERC2* gene began its evolutionary odyssey, and we propose that duplications of this gene first formed duplicons flanking a *NIPA1-NIPA2-CYFIP1-GCP5* cassette at a position equivalent to BP3 (fig. 7). Subsequently, the ~250-kb

four-gene unique cassette (with all required *cis* regulatory elements) and flanking *HERC2* duplicons were transposed by a duplicon-mediated process in an ancestral primate to a site ~4 Mb away, on the other side of the imprinted gene domain. Here, the flanking *HERC2* duplicons would now have formed the BP1 and BP2 domains, as found in human (fig. 7). This transposition may have involved *HERC2* duplicons directly, as supported by the location of a *HERC2* duplicon in BAC 26F2 immediately adjacent to *NIPA1* at BP1 (data not shown). Alternatively, other duplicons have been added and interspersed with *HERC2* duplicons at unknown times during primate evolution (Buiting et al. 1999; Christian et al. 1999; Pujana et al. 2001) and may have contributed to the genomic transposition. Genomic studies of primates will help determine the timing of these events and mechanisms, although secondary rearrangements within and between duplicated sequences in different extant primate species might complicate interpretation of the exact evolutionary events. Nevertheless, it is clear that an evolutionary genetic instability has been conferred on this domain by the origin and expansion of large blocks of duplicated DNA sequences, now mirrored by the events that mediate chromosome rearrangements in genomic diseases involving 15q11-q13.

Acknowledgments

Electronic-Database Information

Accession numbers and URLs for data presented herein are as follows:

Biological Software, Institut Pasteur, http://bioweb.pasteur.fr/ intro-uk.html (for the CLUSTAL W identity/similarity matrix program and the drawtree program to plot unrooted tree diagrams)
Fugu BLAST Server, http://fugu.hgmp.mrc.ac.uk/blast/blast.cgi (for BLAST searches to identify the *Fugu p, Herc2, Nipa1, Nipa2, Cyfip1,* and *Gcp5* gene orthologs)
GenBank, http://www.ncbi.nlm.nih.gov/Genbank/ (for mouse *Nipa1* cDNA [accession number AY098645], for chicken *Nipa2* cDNA [accession number AY099502], for human

NIPA1 cDNA [accession number BK001020], for human *NIPA2* cDNA [accession number BK001120], for mouse *Nipa2* cDNA [accession number BK001121], and for *Xenopus Nipa2* cDNA [accession number BK001125])

GeneMap '98, http://www.ncbi.nlm.nih.gov/genemap98/

NCBI BLAST, http://www.ncbi.nlm.nih.gov/BLAST/ (for BLAST searches)

Online Mendelian Inheritance in Man (OMIM),http://www.ncbi.nlm.nih.gov/Omim/ (for PWS, AS, and SPG6)

TMHMM Server v. 2.0, http://www.cbs.dtu.dk/services/TMHMM-2.0/ (for TMH prediction)

Trace Archive Database, http://www.ncbi.nlm.nih.gov/blast/mmtrace.html (for mouse genome sequences)

References

Amos-Landgraf JM, Ji Y, Wayne G, Depinet T, Wandstrat SB, Daniel JD, Rogan PK, Schwartz S, Nicholls RD (1999) Chromosome breakage in the Prader-Willi and Angelman syndromes involves recombination between large, transcribed repeats at proximal and distal breakpoints. Am J Hum Genet 65:370–386

Boccaccio I, Glatt-Deeley H, Watrin F, Roëckel N, Lalande M, Muscatelli F (1999) The human MAGEL2 gene and its mouse homologue are paternally expressed and mapped to the Prader-Willi region. Hum Mol Genet 8:2497–2505

Buiting K, Korner C, Ulrich B, Wahle E, Horsthemke B (1999) The human gene for the poly(A)-specific ribonuclease (PARN) maps to 16p13 and has a truncated copy in the Prader-Willi/Angelman syndrome region on 15q11→q13. Cytogenet Cell Genet 87:125–131

Buiting K, Saitoh S, Gross S, Dittrich B, Schwartz S, Nicholls RD, Horsthemke B (1995) Inherited microdeletions in the Angelman and Prader-Willi syndromes define an imprinting centre on human chromosome 15. Nat Genet 9:395–400

Butler MG, Bittel DC, Kibiryeva N, Talebizadeh Z, Thompson T. Behavioral differences among subjects with Prader-Willi syndrome and type I and type II deletions and maternal disomy. Pediatrics, in press

Butler MG, Bittel D, Talebizadeh Z (2002) Prader-Willi syndrome and a deletion/duplication within the 15q11-q13 region. J Med Genet 39:202–204

Cavaillé J, Buiting K, Kiefmann M, Lalande M, Brannan CI, Horsthemke B, Bachellerie JP, Brosius J (2000) Identification of brain-specific and imprinted small nucleolar RNA genes exhibiting an unusual genomic organization. Proc Natl Acad Sci USA 97:14311–14316

Chai JH, Locke DP, Ohta T, Greally JM, Nicholls RD (2001) Retrotransposed genes such as Frat3 in the mouse chromosome 7C Prader-Willi syndrome region acquire the imprinted status of their insertion site. Mamm Genome 12:813–821

Cheng SD, Spinner NB, Zackai EH, Knoll JH (1994) Cytogenetic and molecular characterization of inverted duplicated chromosomes 15 from 11 patients. Am J Hum Genet 55:753–759

Chess A, Simon I, Cedar H, Axel R (1994) Allelic inactivation regulates olfactory receptor gene expression. Cell 78:823–834

Chluba-de Tapia J, de Tapia M, Jaggin V, Eberle AN (1997) Cloning of a human multispanning membrane protein cDNA: evidence for a new protein family. Gene 197:195–204

Christian SL, Fantes JA, Mewborn SK, Huang B, Ledbetter DH (1999) Large genomic duplicons map to sites of instability in the Prader-Willi/Angelman syndrome chromosome region (15q11-q13). Hum Mol Genet 8:1025–1037

Clayton-Smith J, Driscoll DJ, Waters MF, Webb T, Andrews T, Malcolm S, Pembrey ME, Nicholls RD (1993) Difference in methylation patterns within the D15S9 region of chromosome 15q11-13 in first cousins with Angelman syndrome and Prader-Willi syndrome. Am J Med Genet 47:683–686

Cornillon S, Pech E, Benghezal M, Ravanel K, Gaynor E, Letourneur F, Bruckert F, Cosson P (2000) Phg1p is a nine-transmembrane protein superfamily member involved in dictyostelium adhesion and phagocytosis. J Biol Chem 275:34287–34292

Crosby AH, Proukakis C (2002) Is the transportation highway the right road for hereditary spastic paraplegia? Am J Hum Genet 71:1009–1016

Culiat CT, Stubbs LJ, Woychik RP, Russell LB, Johnson DK, Rinchik EM (1995) Deficiency of the β_3 subunit of the type A γ-aminobutyric acid receptor causes cleft palate in mice. Nat Genet 11:344–346

de los Santos T, Schweizer J, Rees CA, Francke U (2000) Small evolutionarily conserved RNA, resembling C/D box small nucleolar RNA, is transcribed from PWCR1, a novel imprinted gene in the Prader-Willi deletion region, which is highly expressed in brain. Am J Hum Genet 67:1067–1082

Dhar M, Webb LS, Smith L, Hauser L, Johnson D, West DB (2000) A novel ATPase on mouse chromosome 7 is a candidate gene for increased body fat. Physiol Genomics 4:93–100

Fantes JA, Mewborn SK, Lese CM, Hedrick J, Brown RL, Dyomin V, Chaganti RS, Christian SL, Ledbetter DH (2002) Organisation of the pericentromeric region of chromosome 15: at least four partial gene copies are amplified in patients with a proximal duplication of 15q. J Med Genet 39:170–177

Fernandez J, Yaman I, Sarnow P, Snider MD, Hatzoglou M (2002) Regulation of internal ribosomal entry site-mediated translation by phosphorylation of the translation initiation factor eIF2α. J Biol Chem 277:19198–19205

Fink JK, Jones SM, Sharp GB, Lange BM, Otterud B, Leppert M (1996) Hereditary spastic paraplegia linked to chromosome 15q: analysis of candidate genes. Neurology 46:835–836

Fink JK, Wu CT, Jones SM, Sharp GB, Lange BM, Lesicki A, Reinglass T, Varvil T, Otterud B, Leppert M (1995) Autosomal dominant familial spastic paraplegia: tight linkage to chromosome 15q. Am J Hum Genet 56:188–192

Gabriel JM, Higgins MJ, Gebuhr TC, Shows TB, Saitoh S, Nicholls RD (1998) A model system to study genomic imprinting of human genes. Proc Natl Acad Sci USA 95:14857–14862

Gabriel JM, Merchant M, Ohta T, Ji Y, Caldwell RG, Ramsey MJ, Tucker JD, Longnecker RM, Nicholls RD (1999) A transgene insertion creating a heritable chromosome deletion mouse model of Prader-Willi and Angelman syndromes. Proc Natl Acad Sci USA 96:9258–9263

Gimelli G, Pujana MA, Patricelli MG, Russo S, Giardino D, Larizza L, Cheung J, Armengol L, Schinzel A, Estivill X, Zuffardi O (2003) Genomic inversions of human chromosome 15q11-q13 in mothers of Angelman syndrome patients with class II (BP2/3) deletions. Hum Mol Genet 12:849–858

Gray TA, Hernandez L, Carey AH, Schaldach MA, Smithwick MJ, Rus K, Marshall Graves JA, Stewart CL, Nicholls RD (2000) The ancient source of a distinct gene family encoding proteins featuring RING and C3H zinc finger motifs with abundant expression in developing brain and nervous system. Genomics 66:76–86

Gray TA, Saitoh S, Nicholls RD (1999) An imprinted, mammalian bicistronic transcript encodes two independent proteins. Proc Natl Acad Sci USA 96:5616–5621

Greally JM, Starr DJ, Hwang S, Song L, Jaarola M, Zemel S (1998) The mouse H19 locus mediates a transition between imprinted and non-imprinted DNA replication patterns. Hum Mol Genet 7:91–95

Hagiwara N, Katarova Z, Siracusa LD, Brilliant MH (2003) Nonneuronal expression of the GABA(A) β3 subunit gene is required for normal palate development in mice. Dev Biol 254:93–101

Henegariu O, Heerema NA, Lowe Wright L, Bray-Ward P, Ward DC, Vance GH (2001) Improvements in cytogenetic slide preparation: controlled chromosome spreading, chemical aging and gradual denaturing. Cytometry 43:101–109

Herzing LB, Kim SJ, Cook EH Jr, Ledbetter DH (2001) The human aminophospholipid-transporting ATPase gene ATP10C maps adjacent to UBE3A and exhibits similar imprinted expression. Am J Hum Genet 68:1501–1505

Hollander GA, Zuklys S, Morel C, Mizoguchi E, Mobisson K, Kimpson S, Terhorst C, Wishart W, Golan DE, Bhan AK, Burakoff SJ (1998) Monoallelic expression of the interleukin-2 locus. Science 279:2118–2121

Homanics GE, Delorey TM, Firestone LL, Quinlan JJ, Handforth A, Harrison NL, Krasowshi MD, Rick CE, Korpi ER, Makela R, Brilliant MH, Hagiwara N, Ferguson C, Snyder K, Olsen RW (1997) Mice devoid of γ-aminobutyrate type A receptor β3 subunit have epilepsy, cleft palate, and hypersensitive behavior. Proc Natl Acad Sci USA 94:4143–4148

Huang B, Crolla JA, Christian SL, Wolf-Ledbetter ME, Macha ME, Papenhausen PN, Ledbetter DH (1997) Refined molecular characterization of the breakpoints in small inv dup(15) chromosomes. Hum Genet 99:11–17

Jay P, Rougeulle C, Massacrier A, Moncla A, Mattei MG, Malzac P, Roeckel N, Taviaux S, Lefranc JL, Cau P, Berta P, Lalande M, Muscatelli F (1997) The human necdin gene, NDN, is maternally imprinted and located in the Prader-Willi syndrome chromosomal region. Nat Genet 17:357–361

Jenuwein T, Allis CD (2001) Translating the histone code. Science 293:1074–1080

Ji Y, Walkowicz MJ, Buiting K, Johnson DK, Tarvin RE, Rinchik EM, Horsthemke B, Stubbs L, Nicholls RD (1999) The ancestral gene for transcribed, low-copy repeats in the Prader-Willi/Angelman region encodes a large protein implicated in protein trafficking, which is deficient in mice with neuromuscular and spermiogenic abnormalities. Hum Mol Genet 8:533–542

Jiang YH, Armstrong D, Albrecht U, Atkins CM, Noebels JL, Eichele G, Sweatt JD, Beaudet AL (1998) Mutation of the Angelman ubiquitin ligase in mice causes increased cytoplasmic p53 and deficits of contextual learning and long-term potentiation. Neuron 21:799–811

Jong MTC, Gray TA, Ji Y, Glenn CC, Saitoh S, Driscoll DJ, Nicholls RD (1999) A novel imprinted gene, encoding a RING zinc-finger protein, and overlapping antisense transcript in the Prader-Willi syndrome critical region. Hum Mol Genet 8:783–793

Kitsberg D, Selig S, Brandeis M, Simon I, Keshet I, Driscoll DJ, Nicholls RD, Cedar H (1993) Allele-specific replication timing of imprinted gene regions. Nature 364:459–463

Knoll JH, Cheng SD, Lalande M (1994) Allele specificity of DNA replication timing in the Angelman/Prader-Willi syndrome imprinted chromosomal region. Nat Genet 6:41–46

Knoll JHM, Lichter P (1994) In situ hybridization to metaphase chromosomes and interphase nuclei. In: Dracopoli NC, Haines JL, Korf BR, Moir DT, Morton CC, Seidman CE, Seidman JG (eds) Current protocols in human genetics, vol 1. John Wiley, New York, pp 4.3.1–4.3.28

Knoll JH, Nicholls RD, Magenis RE, Glatt K, Graham JM Jr, Kaplan L, Lalande M (1990) Angelman syndrome: three molecular classes identified with chromosome 15q11q13-specific DNA markers. Am J Hum Genet 47:149–155

Kobayashi K, Kuroda S, Fukata M, Nakamura T, Nagase T, Nomura N, Matsuura Y, Yoshida-Kubomura N, Iwamatsu A, Kaibuchi K (1998) p140Sra-1 (specifically Rac1-associated protein) is a novel specific target for Rac1 small GTPase. J Biol Chem 273:291–295

Köster F, Schinke B, Niemann S, Hermans-Borgmeyer I (1998) Identification of shyc, a novel gene expressed in the murine developing and adult nervous system. Neurosci Letters 252:69–71

Leana-Cox J, Jenkins L, Palmer CG, Plattner R, Sheppard L, Flejter WL, Zackowski J, Tsien F, Schwartz S (1994) Molecular cytogenetic analysis of inv dup(15) chromosomes, using probes specific for the Prader-Willi/Angelman syndrome region: clinical implications. Am J Hum Genet 54:748–756

Lee S, Kozlov S, Hernandez L, Chamberlain SJ, Brannan CI, Stewart CL, Wevrick R (2000) Expression and imprinting of MAGEL2 suggest a role in Prader-Willi syndrome and the homologous murine imprinting phenotype. Hum Mol Genet 9:1813–1819

Lehman AL, Nakatsu Y, Ching A, Bronson RT, Oakey RJ, Keiper-Hrynko N, Finger JN, Durham-Pierre (1998) A very large protein with diverse functional motifs is deficient in rjs (runty, jerky, sterile) mice. Proc Natl Acad Sci USA 95:9436–9441

Locke DP, Yavor AM, Lehoczky J, Chang J, Dewar K, Zhao S, Nicholls RD, Schwartz S, Eichler EE (2001) Structure and evolution of genomic duplication in 15q11-q13. Am J Hum Genet 69:179

Lossie AC, Whitney MM, Amidon D, Dong HJ, Chen P, Theriaque D, Huston A, Nicholls RD, Zori RT, Williams CA, Driscoll DJ (2001) Distinct phenotypes distinguish the molecular classes of Angelman syndrome. J Med Genet 38:834–845

Lunyak VV, Burgess R, Prefontaine GG, Nelson C, Sze SH,

Chenoweth J, Schwartz P, Pevzner PA, Glass C, Mandel G, Rosenfeld MG (2002) Corepressor-dependent silencing of chromosomal regions encoding neuronal genes. Science 298: 1747–1752

MacDonald HR, Wevrick R (1997) The necdin gene is deleted in Prader-Willi syndrome and is imprinted in human and mouse. Hum Mol Genet 6:1873–1878

Meguro M, Kashiwagi A, Mitsuya K, Nakao M, Kondo I, Saitoh S, Oshimura M (2001) A novel maternally expressed gene, ATP10C, encodes a putative aminophospholipid translocase associated with Angelman syndrome. Nat Genet 28: 19–20

Morales J, Hiesinger PR, Schroeder AJ, Kume K, Verstreken P, Jackson FR, Nelson DL, Hassan BA (2002) *Drosophila* fragile X protein, DFXR, regulates neuronal morphology and function in the brain. Neuron 34:961–972

Morris DR, Geballe AP (2000) Upstream open reading frames as regulators of mRNA translation. Mol Cell Biol 20:8635–8642

Mostoslavsky R, Singh N, Tenzen T, Goldmit M, Gabay C, Elizur S, Qi P, Reubinoff BE, Chess A, Cedar H, Bergman Y (2001) Asynchronous replication and allelic exclusion in the immune system. Nature 414:221–225

Murphy SM, Preble AM, Patel UK, O'Connell KL, Dias DP, Moritz M, Agard D, Stults JT, Stearns T (2001) GCP5 and GCP6: two new members of the human γ-tubulin complex. Mol Biol Cell 12:3340–3352

Ng J, Nardine T, Harms M, Tzu J, Goldstein A, Sun Y, Dietzl G, Dickson BJ, Luo L (2002) Rac function and regulation during *Drosophila* development. Nature 416:438–442

Nicholls RD (1999) Incriminating gene suspects, Prader-Willi style. Nat Genet 23:132–134

Nicholls RD, Gottlieb W, Russell LB, Davda M, Horsthemke, B, Rinchik EM (1993) Evaluation of potential models for imprinted and nonimprinted components of human chromosome 15q11-q13 syndromes by fine-structure homology mapping in the mouse. Proc Natl Acad Sci USA 90:2050–2054

Nicholls RD, Knepper JL (2001) Genome organization, function and imprinting in Prader-Willi and Angelman syndromes. Annu Rev Genomics Hum Genet 2:153–175

Osborne LR, Li M, Pober B, Chitayat D, Bodurtha J, Mandel A, Costa T, Grebe T, Cox S, Tsui LC, Scherer SM (2001) A 1.5 million-base pair inversion polymorphism in families with Williams-Beuren syndrome. Nat Genet 29:321–325

Pan CJ, Lei KJ, Annabi B, Hemrika W, Chou JY (1998) Transmembrane topology of glucose-6-phosphatase. J Biol Chem 273:6144–6148

Proudfoot NJ, Furger A, Dye MJ (2002) Integrating mRNA processing with transcription. Cell 108:501–512

Pujana MA, Nadal M, Gratacos M, Peral B, Csiszar K, Gonzalez-Sarmiento R, Sumoy L, Estivill X (2001) Additional complexity on human chromosome 15q: identification of a set of newly recognized duplicons (LCR15) on 15q11-q13, 15q24, and 15q26. Genome Res 11:98–111

Qiu Z, Nicoll DA, Philipson KD (2001) Helix packing of functionally important regions of the cardiac Na(+)-Ca(2+) exchanger. J Biol Chem 276:194–199

Rainier S, Chai J-H, Tokarz D, Nicholls RD, Fink JK (2003) *NIPA1* gene mutations cause autosomal dominant hereditary spastic paraplegia (SPG6) Am J Hum Genet 73:967–971 [in this issue]

Rinchik EM, Stoye JP, Frankel WN, Coffin J, Kwon BS, Russell LB (1993) Molecular analysis of viable spontaneous and radiation-induced albino (*c*)-locus mutations in the mouse. Mutat Res 286:199–207

Ritchie RJ, Mattei MG, Lalande M (1998) A large polymorphic repeat in the pericentromeric region of human chromosome 15q contains three partial gene duplications. Hum Mol Genet 7:1253–1260

Roberts SE, Dennis NR, Browne CE, Willatt L, Woods CG, Cross I, Jacobs PA, Thomas NS (2002) Characterisation of interstitial duplications and triplications of chromosome 15q11-q13. Hum Genet 110:227–234

Runte M, Huttenhofer A, Gross S, Kiefmann M, Horsthemke B, Buiting K (2001) The IC-SNURF-SNRPN transcript serves as a host for multiple small nucleolar RNA species and as an antisense RNA for UBE3A. Hum Mol Genet 10: 2687–2700

Saitoh S, Buiting K, Rogan PK, Buxton JL, Driscoll DJ, Arnemann J, Konig R, Malcolm S, Horsthemke B, Nicholls RD (1996) Minimal definition of the imprinting center and fixation of chromosome 15q11-q13 epigenotype by imprinting mutations. Proc Natl Acad Sci USA 93:7811–7815

Schenck A, Bardoni B, Moro A, Bagni C, Mandel JL (2001) A highly conserved protein family interacting with the fragile X mental retardation protein (FMRP) and displaying selective interactions with FMRP-related proteins FXR1P and FXR2P. Proc Natl Acad Sci USA 98:8844–8849

Schimmöller F, Diaz E, Muhlbauer B, Pfeffer SR (1998) Characterization of a 76 kDa endosomal, multispanning membrane protein that is highly conserved throughout evolution. Gene 216:311–318

Sheets MD, Ogg SC, Wickens MP (1990) Point mutations in AAUAAA and the poly (A) addition site: effects on the accuracy and efficiency of cleavage and polyadenylation in vitro. Nucleic Acids Res 18:5799–5805

Simon I, Tenzen T, Reubinoff BE, Hillman D, McCarrey JR, Cedar H (1999) Asynchronous replication of imprinted genes is established in the gametes and maintained during development. Nature 401:929–932

Spritz RA, Bailin T, Nicholls RD, Lee ST, Park SK, Mascari MJ, Butler MG (1997) Hypopigmentation in the Prader-Willi syndrome correlates with P gene deletion but not with haplotype of the hemizygous P allele. Am J Med Genet 71: 57–62

Sugasawa T, Lenzen G, Simon S, Hidaka J, Cahen A, Guillaume JL, Camoin L, Strosberg AD, Nahmias C (2001) The iodocyanopindolol and SM-11044 binding protein belongs to the TM9SF multispanning membrane protein superfamily. Gene 273:227–237

Thompson JD, Higgins DG, Gibson TJ (1994) CLUSTAL W: improving the sensitivity of progressive multiple sequence alignment through sequence weighting, positions-specific gap penalties and weight matrix choice. Nucleic Acids Res 22:4673–4680

Turner BM (2002) Cellular memory and the histone code. Cell 111:285–291

Walkowicz M, Ji Y, Ren X, Horsthemke B, Russell LB, Johnson D, Rinchik EM, Nicholls RD, Stubbs L (1999) Molecular

characterization of radiation- and chemically induced mutations associated with neuromuscular tremors, runting, juvenile lethality, and sperm defects in jdf2 mice. Mamm Genome 10:870–878

Worthington MT, Pelo JW, Sachedina MA, Applegate JL, Arseneau KO, Pizarro TT (2002) RNA binding properties of the AU-rich element-binding recombinant Nup475/TIS11/tristetraprolin protein. J Biol Chem 277:48558–48564

Wu M, Rinchik EM, Johnson DK (2000) An integrated deletion and physical map encompassing l71Rl, a chromosome 7 locus required for peri-implantation survival in the mouse. Genomics 67:228–231

Zhao J, Hyman L, Moore C (1999) Formation of mRNA 3′ ends in eukaryotes: mechanism, regulation, and interelationships with other steps in mRNA synthesis. Microbiol Mol Biol Rev 63:405–445